REFERENCE 145

L. B. ENGLE, G. E. HANSEN, AND H. C. PAXTON, "REACTIVITY CONTRIBUTIONS OF VARIOUS MATERIALS IN TOPSY, GODIVA, AND JEZEBEL," NUCL. SCI. ENG. 8: 543-569 (1960).

NUCLEAR SCIENCE and ENGINEERING

THE JOURNAL OF THE AMERICAN NUCLEAR SOCIETY

VOLUME 8, NUMBER 6, December 1960

NUCLEAR SCIENCE AND ENGINEERING: 8, 543–569 (1960)

Reactivity Contributions of Various Materials in Topsy, Godiva, and Jezebel*

L. B. ENGLE, G. E. HANSEN, AND H. C. PAXTON

University of California, Los Alamos Scientific Laboratory, Los Alamos, New Mexico

Received June 6, 1960

This report brings together an extensive accumulation of reactivity contribution data for the various critical assemblies at Pajarito. Corresponding values of effective absorption and transport cross sections are derived, and relationships between critical mass and volume fraction of diluents are obtained in terms of these cross sections. In some favorable cases, inelastic scattering contributions to the effective absorption cross sections are estimated.

I. EXPERIMENTAL

Within the past ten years, information on the effects of local additions of materials has been accumulated for a number of Pajarito critical assemblies. This report presents results of material replacement measurements on five critical assemblies, four in which the active material is Oy (~94) metal,[1] and one of δ-phase Pu metal. One of the assemblies (Topsy Oy-U) is enriched uranium in a thick natural uranium reflector, a variant had a core at one-half normal density, and in another case (Topsy Oy-Ni), thick nickel was substituted for the uranium reflector. Another (Godiva) is enriched uranium without reflector, and the final assembly is bare δ-phase plutonium. Reported by Linenberger *et al.* (*1*), are series of similar results for assemblies with cores effectively of Oy (93.15%) $H_{2.97}C_{1.11}O_{0.25}$ and reflectors of thick U and of thick Ni.

METHOD

A reactivity contribution measurement is the determination of the reactivity change when a small cavity within the system is filled by a sample of the material of interest. Actually, the difference in control rod settings for delayed critical operation with the cavity filled and empty is observed. As changes are made manually, disassembly of the system is required between such observations. By means of a control rod calibration curve, the result is converted to units of cents per mole of perturbing material, where 100 cents is the reactivity interval between delayed and prompt critical (*2*).

Consistency of standards (cavity empty) which bracket each determination with the sample in place, is required for an acceptable measurement. With the assembly reproducing satisfactorily, drifts in series of standards correlate with changes in ambient temperature (for Jezebel, constant temperature was maintained). At the operating level for these tests (~1 w), self-heating of the oralloy assemblies is negligible.

TOPSY MEASUREMENTS

Three of the critical assemblies to be considered were set up on the Topsy machine (*3*). The system in which the more complete series of replacement measurements was made consisted of a roughly spherical core built up of $\frac{1}{2}$-in.^{3} units of Oy, surrounded intimately by a full density U reflector of 9-in. average thickness (effectively almost infinite). The critical mass was 17.4 kg Oy (94.1%) at an average core density of 18.7 g/cm^3. The replacements generally were made in $\frac{1}{2}$-in.^{3} cavities in a layer centered about $\frac{1}{2}$ in. below the median plane of the assembly, although Oy, Pu, and U checks were made in $\frac{1}{2}$ in. diam × $\frac{1}{2}$ in. long cylindrical cavities in the radial "glory hole" of the assembly. Most samples were $\frac{1}{2}$-in. cubes or $\frac{1}{2}$ in. diam × $\frac{1}{2}$ in. cylinders of full density metal or of pressed powder,

* Work done under the auspices of the U. S. Atomic Energy Commission.

[1] Oralloy, abbreviated Oy, signifies uranium enriched in U^{235}. Oy (~94) implies about 94 wt % U^{235}.

and wherever possible were of high-purity material. Results of measurements on this Oy-U assembly are presented in Table I. The few existing data for a similar assembly with core at 50% normal density are given in Table II.

The other Topsy assembly had a similar "pseudo-spherical" Oy core in a full density Ni reflector of about $8\frac{3}{4}$ in. average thickness. In this case, the critical mass was 21.2 kg Oy (94%) at an average density of 18.7 g/cm^3. Samples were $\frac{1}{2}$-in. cubes of

TABLE I

Topsy Oy - Thick U Assembly (Oy Radius = 2.39 in.)

Reactivity Contributions Δk of Various Materials in Cents/mole

1/2 in. Cubic Samples Unless Noted Otherwise ("Radius" Refers to Position of Sample Center)

Radius (in.)	0.44 (0.51)*	0.67 (0.715)*	1.09 (1.12)*	1.56 (1.58)*	2.05* (2.06)** (2.04)	2.50	2.54* (2.55)*	2.93	3.54	4.30	4.71	5.29
Li_2SO_4[a]	-0.5											
$Li_2^6SO_4$[a] (89.42%)	-99.6											
Be	8.8		10.7	11.8	12.6		8.7		2.5			0.3
BeO	10.7			20.3	23.0		17.0					
B[a]	-9.6	-8.4	-5.0	0.0	4.7**	4.4			0.4			-0.1
C	2.9	4.2	6.1	9.8	11.5		8.7	5.6	2.8	1.2	0.8	0.4
CH_2	125	120	112	91	65		32	14.4	2.3	-1.7	-1.9	-1.9
CD_2 (98.34%)	46.3											
CF_2	11.9		22.0		39.7							
Mg	2.1						9.7					
MgF_2[a]	14.2		27.0		39.5		29.5					
Al	1.4	2.0	5.5	8.3	10.8**	9.3	8.5	5.4	2.7	1.3	0.6	0.5
Al_2O_3[a]	9.3		28.5									
S[a]	-7.2		-2.5		6.9							
Ca[b]	-5											
Ti	-0.7				10.6							
V	1.2		6.5		14.8		11.6					
Cr	-0.5				11.8		8.5					
Fe	-0.45*	0.68*	3.67*	7.54*	10.8		8.2					
Mn	0.2		5.4		13.1**	10.8	10.0	6.1	3.0	1.7		
Co	-1.2		4.1		12.7		9.3					
Ni	-4.38*	-3.09*	0.88*	5.87*	10.4	9.4	8.4					
Cu	-1.67*	-0.50*	3.04*	7.84*	11.8		9.3					
Zn	-2.88*	-1.13*	2.75*	7.98*	12.7		9.8					
Ga	-2.3		4.0		13.0							
Ge[c]	-2.7											
As[a]	0.0		6.9		19.2		15.0					
Zr[b]	-0.6				19.0		15.7					
Nb[a]	-5.1	-1.8	3.8	10.9	16.4	14.9		8.6	3.9	2.0	1.4	0.8
Mo[a]	-1.5				20.6	17.9	16.4	10.3	4.9	1.8	1.5	
Rh[a]	-10.9		-4.2		11.4**	10.3		5.4	2.0	0.7		0.1
Pd[a]	-7.8		-0.3		13.2		10.7					
Ag	-14.9		-7.7		9.4		7.5					
Cd	-6.9		0.4		13.8		11.6					
In[a]	-21.0		-11.7		7.2**	7.2		3.7	1.7	0.5	-0.2	
Sn	-2.5				15.6		11.6					
Sb	-11.3		-1.2		12.0		9.1					
I[a]	-10.3											
La[b]	-0.0											
Ce	-2.5											
Nd[b]	-6.0											

TABLE I (*Continued*)

Topsy Oy - Thick U Assembly (Oy Radius = 2.39 in.)

Reactivity Contributions Δk of Various Materials in Cents/mole

1/2 in. Cubic Samples Unless Noted Otherwise ("Radius" Refers to Position of Sample Center)

Radius (in.)	0.44 (0.51)*	0.67 (0.715)*	1.09 (1.12)*	1.56 (1.58)*	2.05 (2.06)* (2.04)**	2.50	2.54 (2.55)*	2.93	3.54	4.30	4.71	5.29
Ta	-13.6		-4.8		12.9	11.6			3.2			0.0
W	-7.7		3.6		18.0		14.4					
Ir[c]	-16.9											
Pt[a]	-7.8		1.8		16.9		13.2					
Au[a]	-12.4		-2.6		13.5	12.2	12.0	6.9	3.1	1.1		0.4
Pb	0.4				21.2		16.3					
Bi	-1.7				22.6		17.0					
Th	-4.8	-2.5*	4.3	13.7	20.2		14.8					
U	24.5*	25.6*	27.3*	30.1*	30.2*	22.1	20.2*	11.9	5.5	2.2	1.5	0.7
Oy (95.4%)	184.6*	178.9*	163.9*	137.9*	105.6*	73.0	68.8*	46.3	26.2	13.9	10.5	6.7
U^{233} (98.2%)	328.1*	314*	284.3*	232.1*	172.1*		108.3*	77.5				
Np^{237}[d]	160±8											
Pu^{239} (98.5%)	377.1*	362.7*	324.5*	259*	187.9*	128	115*	81.3	44.0	22.8	17.2	10.6
Pu^{240}[e]	268*											

[a] Pressed powder (1/2 in. cube or cylinder).

[b] Small irregular sample.

[c] Powder in 1/2 in. diam. x 1/2 in. (~0.5 g) Al can.

[d] 0.3 g sample at r = 0.32 in.

[e] From Pu samples containing 0 - 6% Pu^{240}.

Note on errors: The estimated probable error of a determination is about ± 0.02 cent/sample. As indicated by the following list of moles per sample, probable errors in cent/mole range from ± 0.1 to ± 0.3 except for extreme cases: Li_2SO_4 -- 0.02; $Li_2^6SO_4$ -- 0.02; Be -- 0.41; BeO -- 0.22; B -- 0.24; C (graphite) -- 0.28; CH_2 (polythene) -- 0.13; CD_2 (polythene) -- 0.10; CF_2 (Teflon) -- 0.09; Mg -- 0.15; MgF_2 -- 0.06; Al -- 0.20; Al_2O_3 -- 0.06; S -- 0.12; Ca -- 0.04; Ti -- 0.15; V -- 0.15; Cr -- 0.20; Fe -- 0.28; Mn -- 0.19; Co -- 0.25; Ni -- 0.31; Cu -- 0.28; Zn -- 0.20; Ga -- 0.17; Ge -- 0.03; As -- 0.12; Zr -- 0.05; Nb -- 0.14; Mo -- 0.15; Rh -- 0.16; Pd -- 0.20; Ag -- 0.18; Cd -- 0.16; In -- 0.13; Sn -- 0.12; Sb -- 0.10; I -- 0.08; La -- 0.02; Ce -- 0.06; Nd -- 0.007; Ta -- 0.14; W -- 0.12; Ir -- 0.03; Pt -- 0.19; Au -- 0.19; Pb -- 0.11; Bi -- 0.09; Th -- 0.06; U -- 0.16; Oy -- 0.16; U^{233} -- 0.12; Pu -- 0.12 mole/sample.

In addition to the normal error, "wild" values occasionally may appear as a result of masked irreproducibility. Although it is believed that most of these cases have been spotted and eliminated by repetition, it is possible that a few values still may be in error by 1 - 2 cents/mole.

TABLE II

Topsy Oy-Thick U Assembly with Core at One-Half Normal Density

1/2 in. Cubic Spaces and 1/2 in. Cubic Oy Units[a]

Radius (in.)	Oy (94) cents/g-atom	Natural U cents/g-atom	Al cents/g-atom
0.374	69.5		
1.273	64.8	7.4	
1.77	60.7		1.2
2.26	55.7	7.6	
2.76	49.8	8.1	2.1
3.26	43.7	8.1	
3.76	37.0	7.5	2.2
3.89 (interface)	35.5	7.2	
4.14	31.3	6.0	
4.55		3.5	1.9
5.98		1.2	0.7

[a] Replacements in the core were made in lattice positions normally occupied by Oy. A few checks near the interface indicated that dependence on type of lattice position is within experimental error.

TABLE III

Topsy Oy - Thick Ni Assembly (Oy Radius = 2.55 in.)

Reactivity Contributions Δk of Various Materials in Cents/Mole

Generally 1/2 in. Cubic Samples[a]

Radius (in.)	0.83	1.09	1.48	1.92	2.39	2.68	2.86	3.12	3.35
B	-6.7								
B^{10} (85%)	-58.7								
C	5.4				13.9				
Al	4.0				13.6				
Tl	3.7				14.4				
Fe	2.5				14.7				
Cu	1.7				15.9				
Ga	3.7				18.1				
Au	-2.9				21.0				
Bi	5.1				26.2				
Th	5.1				27.2				
Ni	-1.9	0.3	5.5	11.3	11.9	9.5	7.1		3.4
U	33.1	35.6	37.3	39.8	35.1	25.5	19.4		9.1
Oy (95%)	186.3	175.2	152.9	122.8	85.8	63.5	49.0	35.4	28.4
U^{233} (98.2%)	320.7	299.2	254.3	197.8	132.4		74.9	55.1	43.9
Pu^{239}	371.9	343.8	290.3	223.0	144.3		80.5	57.9	45.7

[a] Samples and estimated probable errors are as described in Table I. Because of fewer repeats, however, there may be a greater possibility of "wild" values.

full density or compacted material, and replacements were made in $\frac{1}{2}$-in.^{3} cavities. The limited set of results for this assembly is summarized in Table III.

Godiva and Jezebel Measurements

Other measurements were made in Godiva, the nearly spherical bare Oy critical assembly (*4*), and in Jezebel, the bare Pu assembly that is described in the companion article by Jarvis *et al.* (*5*). The critical mass of Godiva is 52.65 kg Oy (93.7%) at an effective density of 18.7 g/cm^3. For Jezebel measurements and the principal series of Godiva measurements, replacements were made in a $\frac{1}{2} \times \frac{1}{2}$-in. cylindrical cavity within the diametral "glory hole." The radial position of the cavity was adjusted by proper arrangement of fillers of various length which fit into the glory hole. Table IV gives the results of this series of tests as functions of distance from the center of Godiva, and Table V gives the corresponding Jezebel data. Samples, in the form of $\frac{1}{2}$ in. diam $\times$ $\frac{1}{2}$ in. cylinders of compact material, generally are of c.p. grade material or the equivalent.

A second group of measurements on Godiva, designed to give more complete information about an apparent periodicity of central reactivity coefficients for odd Z – odd A elements as a function of Z, is reported in Section IV. Finally, transport effects of fissionable materials, deduced from reactivity coefficients at the Godiva surface, are given in Appendix I.

II. REDUCTION OF DATA

Generally, the replacement samples (x) used for the collection of data, $\Delta k(r, x)$, given in Tables I, II, III, IV, and V, consisted of normal density $\frac{1}{2}$-in. cubes or cylinders. This sample size is sufficiently large to permit accurate reactivity change measurements, yet not so large as to introduce serious perturbations in the neutron distribution within the critical assembly. The small corrections to the observed reactivity contributions which remove the effects of these perturbations (henceforth called "sample size" corrections) have been computed by the methods given in the preceding paper (*6*) and the resulting reactivity coefficients,

$$\Delta k_0(r, x)$$

are presented in Tables VI, VII, VIII, and IX. Radial variations for selected materials in Topsy-U and Godiva are shown in Figs. 1 and 2, and similar curves for Jezebel are given by Jarvis *et al.* (*5*).

TABLE IV

Godiva Bare Oy Assembly (Oy Radius = 3.44 in.)

Reactivity Contributions Δk of Various Materials in Cents/Mole

1/2 in. Cylindrical Samples

Radius (in.)	0.030	1.242	1.930	2.512	3.142	3.206
Be	6.7	9.4	11.6	10.8	9.4	
B[a]	-6.3	-0.7	4.9	8.0	7.9	
B^{10} [a] (85%)	-42.1	-27.3	-12.0	-0.1	6.6	6.2
C	2.2	5.0	9.0	10.4	9.7	
CH_2	88.6	76.6	62.0	43.6	24.5	
Al	0.4	4.6	9.3	9.9		8.1
Fe	-0.1	3.9	8.2	10.6		9.0
Co	-0.5		9.7	12.3	11.1	
Ni	-4.0	2.0	8.0	10.7		9.6
Cu	-1.6	4.1	9.3	11.7		10.5
Zn	-2.3	4.5	9.0	11.7		11.6
Ag	-9.2		8.4	14.1	13.7	
W	-5.3					
Au	-6.7	2.2	11.6	17.8	17.8	
Bi	-1.5		16.6	21.8	19.8	
Th	-1.2	8.7	18.8	21.6		20.0
U	21.9		29.0	28.1	22.6	21.2
Oy (93.7%)	135.5	109.7	84.2	58.6	33.2	30.6
Pu^{239}	279.6	220.4	155.4	100.2		42.6
Pu^{240}	168±17					

[a] Powder in 1/2 in. diam. x 1/2 in. (~0.5 g) Al can.

Note on errors: The estimated probable error of a determination is about ± 0.025 cents/sample. From the following list of moles/sample, it is seen that for most materials the probable errors in cents/mole range from ± 0.1 to ± 0.3: Be -- 0.32; B -- 0.24; B^{10} -- 0.27; C (graphite) -- 0.21; CH_2 (polythene) -- 0.10; Al -- 0.16; Fe -- 0.22; Co -- 0.23; Ni -- 0.24; Cu -- 0.22; Zn -- 0.18; Ag -- 0.15; Au -- 0.16; Bi -- 0.07; Th -- 0.08; U -- 0.12; Oy -- 0.12; Pu -- 0.09 mole/sample.

As for Topsy, the possibility of an occasional "wild" value in error by 1 - 2 cents/mole cannot be excluded.

One-Group, or Integral Absorption and Transport Cross Sections

With the major exceptions of hydrogenous materials, the functions $\Delta k_0(r, x)$, for Godiva, Topsy, and Jezebel cores, are given very closely by equations of the form

$$\Delta k_0(r, x) = -\sigma_a(x) f_0(r) + \sigma_{tr}(x) f_1(r) \qquad \text{(II-1)}$$

where $f_0(r)$ and $f_1(r)$ are functions of radius alone as would be expected from one-group diffusion theory. However, the one-group relations

$$f_0(r) = c\,(\sin kr - kr)^2, \text{ and}$$

$$f_1(r) = c \cdot 3 \left\{ \frac{[(\nu - 1)\Sigma_f - \Sigma_c]}{k^2} \frac{d}{dr} \frac{\sin kr}{kr} \right\}^2 \qquad \text{(II-2)}$$

hold only in the region $r > 0$. In these expressions, $k \cong 0.29$ cm^{-1} for Oy (93) and ~0.38 for Pu^{239}, and $(\nu - 1)\Sigma_f - \Sigma_c \cong 0.085$ cm^{-1} for Oy or ~0.149 cm^{-1} for Pu. As a rule, then, measurements at many different radial positions disclose only two numbers characteristic of (x); viz., $\sigma_a(x)$ and $\sigma_{tr}(x)$. With a one-energy-group model, if the constant c is chosen as the central reactivity change associated with a one-barn capture cross section, then $\sigma_a(x)$ and $\sigma_{tr}(x)$ would represent, respectively, capture and transport cross sections of (x) in barns. In an actual case, processes which transfer neutrons from one energy to another also contribute to reactivity changes, and unit capture in different energy regions gives different reactivity contributions. Nevertheless, it is convenient to assign a value to c and obtain numerical values of $\sigma_a(x)$ and $\sigma_{tr}(x)$. Such values then represent a condensed version of the corrected replacement data. We have chosen the constants c (Godiva) and c (Topsy) such that $-\sigma_a(\text{Oy}) \cong$

TABLE V

Jezebel Bare Pu Assembly (Radius 2.48 in.)

Reactivity Contributions Δk of Various Materials in Cents/Mole

1/2 in. Cylindrical Samples Unless Noted Otherwise

Radius (in.)	0.00	0.72	1.22	1.78	2.28
Be	13.1	34.8	61.4	77.3	67.1
BeO	5.25	48.4	104.8	143.3	134.0
B^{10} (96%)	-199.2			-2.6[a]	
C	-5.8	18.2	46.6	71.35	68.0
CH_2	100.7	133.4	174.2	189.8	151.1
CD_2	-14.7	46.1	125.2	190.0	183.7
CF_2	-36.8		155.3	224.8[a]	
Al	-11.9	15.0	48.6	77.0	71.3
Si	-13.7	11.1	49.8	77.3	72.7
SiO_2	-31.3	47.9	146.9	221.0	211.8
S	-59.0			36.9[a]	
Ti	-21.8	12.6	49.2	78.6	73.5
TiN[b]	-40.8	26.9	71.2	147.6	130.7
V[b]	-13.0	20.2	60.1	89.9	87.8
Fe	-18.1	10.1	45.9	76.0	73.5
Co	-20.6	10.2	50.0	87.5	79.7
Ni	-40.2	-6.3	39.0	76.8	78.0
Cu	-27.5	6.3	46.2	84.0	83.9
Zn	-33.9	1.2	46.4	90.4	84.8
Zr[b]	-30.0	27.5	70.3	138.6	133.7
Mo	-37.0	6.4	68.0	118.8	115.3
Ag	-78.2	-27.0	37.1	91.8	95.4
Cd	-55.0	-6.6	58.6	103.6	108.3
Sn	-36.6	4.6	65.4	106.0	108.0
La	-30.5			101.5[a]	
Ce	-28.2 (?)			118.7[a]	
Dy_2O_3[b]	-175.0				
Ho_2O_3[b]	-282.1			440.4	
Yb_2O_3[b]	-156.5				
Ta	-84.1	-27.4	50.5	114.1	121.1
W	-60.9	-6.2	67.4	125.3	129.1
Au	-73.0	-16.1	53.6	121.0	125.9
Bi	-19.7	34.0	99.8	154.3	147.1
Th	-54.4	13.9	88.6	154.2	149.1
U (normal)	94.4	134.4	180.0, 173.6	200.3	172.1
U^{233} (98.2%)	1227			642.7	
Oy (93.44)	676.9	632.5	547.4	407.2	251.6
Np^{237}[b]	669				
Pu (95.3% Pu^{239})	1438.7(1429[c])	1283.8	1028.1	675.8(678.1[c])	372.8

[a] Measured at r = 1.72 in. instead of 1.78 in.
[b] Small sample.
[c] Sample 1/8 in. thick x 1/2 in. diam.

Note: Samples c.p. grade or better; probable error ~0.3 cents/g-atom for standard-size samples, except 0.4% for Pu and Oy; few "wild" values noted.

TABLE VI

Topsy Oy - Thick U Assembly (Oy Radius = 2.39 in.)

Reactivity Coefficients Δk_o of Various Elements in Cents/g-atom

Radius (in.)	0.00	0.44 (0.51)*	0.67 (0.715)*	1.09 (1.12)*	1.56 (1.58)*	2.05 (2.06)** (2.04)**	2.50	2.54 (2.55)*	2.93	3.54	4.30
H[a]	67.6	65.9	62.6	57.4	44.4	29.9		12.3	5.6	0	-1.4
D[b]	24.0	23.6									
Li	-2.4	-1.2									
Li^6	-130.4	-125.3									
Be	9.2	9.5		10.9	11.4	11.7		7.8		2.2	
B	-12.2	-11.0	-9.9	-6.7	-2.0	2.6	3.0			0.0	
C	2.4	3.0	4.1	5.5	8.6	9.8		7.4	4.8	2.4	1.0
O[c]	1.4	2.1		5.1	7.8	9.4		7.5			
F[d]	4.0	4.7		7.4		12.2					
Mg	1.4	2.0						7.9			
Al	0.7	1.3	1.7	4.7	6.8	8.8**	7.7	7.0	4.5	2.2	1.1
S	-8.9	-8.2		-4.1		4.2**					
Ca	-6.6	-5.8									
Ti	-1.9	-1.1				8.3					
V	0.0	1.0		5.3		11.9		9.4			
Cr	-1.7	-0.8				9.7		5.9			
Fe	-2.2	-0.1*	0.1*	2.7*	6.1*	8.9		6.8			
Mn	-1.0	-0.1		4.3		10.6**	8.8	8.1	4.9	2.4	1.5
Co	-2.5	-1.6		2.9		10.3		7.6			
Ni	-7.3	-5.3*	-4.1*	-0.5*	4.1*	8.3	7.9	7.0			
Cu	-3.9	-2.3*	-1.3*	1.8*	6.1*	9.7		7.9			
Zn	-5.2	-3.7*	-2.1*	1.2*	5.8*	10.1		8.0			
Ga	-4.0	-2.9		2.5		10.2					
Ge	-4.5	-3.3									
As	-2.0	-0.5		5.2		15.6		12.3			
Zr	-2.4	-1.1				14.6		12.4			
Nb	-7.5	-6.2	-3.2	1.6	7.8	12.6	12.1		6.9	3.1	1.6
Mo	-3.5	-2.1				16.9	15.2	13.9	8.8	4.1	1.4
Rh	-14.1	-12.5		-6.6		7.9**	7.9		4.0	1.3	0.4
Pd	-10.3	-9.1		-2.3		10.1		8.7			
Ag	-18.0	-16.7		-10.3		6.0		3.0			
Cd	-9.5	-8.0		-1.6		10.4		9.3			
In	-25.8	-23.8		-15.2		2.9**	4.5		2.1	0.9	0.2
Sn	-4.4	-3.2				12.2		9.1			
Sb	-14.5	-13.0		-3.8		7.9		6.4			
I	-13.5	-11.9									
La	-1.8	-0.5									
Ce	-4.5	-7.2									
Ta	-17.2	-15.6		-7.8		8.5	8.6			2.3	
W	-10.8	-8.9		1.2		13.7		11.5			
Ir	-21.3	-19.2									
Pt	-10.7	-9.1		-0.3		13.7		11.0			
Au	-15.8	-14.0		-4.9		10.0	9.9	9.8	5.5	2.4	0.8
Pb	-1.5	-0.0				17.2		13.3			
Bi	-4.1	-2.5				18.0		13.5			
Th	-7.6	-5.9		1.9	9.2	15.7		11.6			
U^{233}	358.7	344.3	329.1*	296.5*	240.2*	175.9*		102.2*	72.8		
U^{235}	208.4	201.1*	194.3*	176.6*	146.6*	110.0*	71.3	67.0*	44.9	25.5	13.6
U^{238}	26.7	27.0*	27.7*	27.6*	28.6*	27.1*	19.6	17.2*	10.1	4.5	1.7
Np^{237}	175±8										
Pu^{239}	402.6	386.3*	371.0*	330.6*	262.2*	188.1*	120.5	106.8*	75.0	40.6	21.2
Pu^{240}	286±14										

[a] From CH_2-C.

[b] From CD_2-C.

[c] Average of values from BeO-Be and Al_2O_3-2Al.

[d] Average of values from CF_2-C and MgF_2-Mg.

TABLE VII

Topsy Oy - Thick Ni Assembly

Reactivity Coefficients Δk_o for Various Elements in Cents/g-atom

Radius (in.)	0	0.83	1.09	1.48	1.92	2.39	2.68	2.86	3.12	3.35
B	-12.2	-8.4								
B^{10}	-89.8	-76.8								
C	2.7	5.0				11.8				
Al	0.9	3.4				11.1				
Ti	0.1	2.9				11.5				
Fe	-1.5	1.7				12.2				
Cu	-3.0	0.8				13.4				
Ga	-1.1	2.7				14.8				
Au	-11.0	-4.8				17.4				
Bi	-1.8	3.6				21.1				
Th	-2.0	3.7				22.6				
Ni	-6.6	-3.0	-1.1	3.7	9.2	9.9	7.9	5.9		2.8
U^{233}	372.8	333.0	309.7	261.1	200.7	130.5		69.5	51.3	41.0
U^{235}	223.5	202.4	189.2	163.1	128.6	86.8	61.3	46.7	34.1	27.5
U^{238}	31.8	33.3	35.0	35.5	36.6	31.5	22.0	16.9		7.8
Pu^{239}	426.0	381.5	351.8	295.1	234.2	141.1		73.2	53.0	41.7

TABLE VIII

Godiva Bare Oy Assembly

Reactivity Coefficients Δk_o for Various Elements in Cents/g-atom

Radius (in.)	0.030	1.242	1.930	2.512	3.142	3.206
H[a]	47.8	38.5	27.7	16.9	7.2	
D[b]	17.8					
Be	7.3	9.4	11.0	9.9	8.4	
B	-6.9	-1.8	3.4	6.4	6.5	
B^{10}	-55.3	-37.6	-19.4	-4.7	4.5	4.1
C	2.4	4.5	7.8	8.9	8.3	
Al	0.5	3.9	7.9	8.2		6.6
Fe	-0.2	3.1	6.9	9.0		7.6
Co	-0.6		8.4	10.7	9.7	
Ni	-4.4	1.0	6.5	9.1		8.2
Cu	-1.8	3.3	7.9	10.0		9.1
Zn	-2.5	3.5	7.3	9.7		9.9
Ag	-10.2		6.1	11.6	11.5	
W	-4.0					
Au	-7.4	0.5	9.3	15.2	15.5	
Bi	-1.7		13.3	17.9	16.2	
Th	-1.4	6.9	15.5	17.7		16.7
U^{235}	149.3	118.8	88.4	59.3	31.9	29.3
U^{238}	24.3		27.6	25.7	19.9	18.6
Pu^{239}	285.2	223.2	154.8	97.9		39.8
Pu^{240}	170±17					

[a] From CH_2-C.
[b] From CD_2-C.

1.78, this being close to the value in barns of

$$[(\nu - 1)\sigma_f - \sigma_c]_{0y}.$$

Similarly c (Jezebel) is chosen such that

$$-\sigma_a(\mathrm{Pu}^{239}) \cong 3.60 \text{ barns},$$

in this case allowing -0.15 barn for inelastic scattering contribution. Table X lists the $\sigma_a(x)$ and $\sigma_{1r}(x)$ values corresponding to the corrected data $\Delta k_0(r, x)$ of Tables VI, VII, VIII, and IX; the empirical functions $f_0(r)$ and $f_1(r)$ are graphed in

TABLE IX

Jezebel Bare Pu Assembly (Radius 2.48 in.)

Reactivity Coefficients Δk_0 of Various Elements in Cents/g-atom

Radius (in.)	0.00	0.72	1.22	1.78	2.28
H[a]	62.8	64.0	66.0	57.4	38.4
D[b]	-5.3	11.2	35.1	53.8	52.6
Be	15.5	35.1	58.6	72.3	62.1
B^{10}	-251			-30.3	
C	-6.9	14.5	39.7	61.9	59.5
N[c]	-22.6	10.6	14.3	55.9	
O[d]	-9.9	12.7	40.3	61.8	61.7
F[e]	-18.4		49.0	71.4	
Al	-14.1	9.4	39.4	64.9	60.8
Si	-16.3	4.5	39.6	64.4	61.5
S	-70.2			23.4	
Ti	-25.9	6.1	37.7	65.0	62.1
V	-15.4	13.7	47.8	74.2	73.4
Fe	-21.5	7.2	37.3	65.6	64.4
Co	-24.5	4.0	42.1	78.0	72.0
Ni	-48.0	-15.6	28.3	65.9	69.3
Cu	-32.7	-0.9	36.9	73.2	74.8
Zn	-40.3	-8.2	34.0	75.6	72.9
Zr	-35.6	16.7	52.6	112.9	110.9
Mo	-44.0	-4.0	55.5	104.7	103.5
Ag	-93.4	-43.8	17.9	73.3	81.5
Cd	-65.5	-20.3	39.8	84.0	91.8
Sn	-43.5	-7.1	48.2	86.3	90.5
La	-36.2			81.8	
Ce	-33.5			97.9	
Dy	-89				
Ho	-153			74	
Yb	-78				
Ta	-100.5	-45.9	30.0	94.5	106.0
W	-82.3	-19.9	46.1	106.9	115.9
Au	-87.2	-32.0	36.2	103.7	112.3
Bi	-23.4	23.5	81.4	129.9	125.2
Th	-64.7	-1.0	65.4	127.2	126.5
U^{233}	1359			671	
U^{235}	804	736	616	435	258
U^{238}	114	146	177	190	160
Np^{237}	789				
Pu^{239}	1592	1408	1111	708	366
Pu^{240}	1038				

[a] From CH_2-C.
[b] From CD_2-C.
[c] From TiN-Ti.
[d] Average of values from BeO-Be and SiO_2-Si.
[e] From CF_2-C.

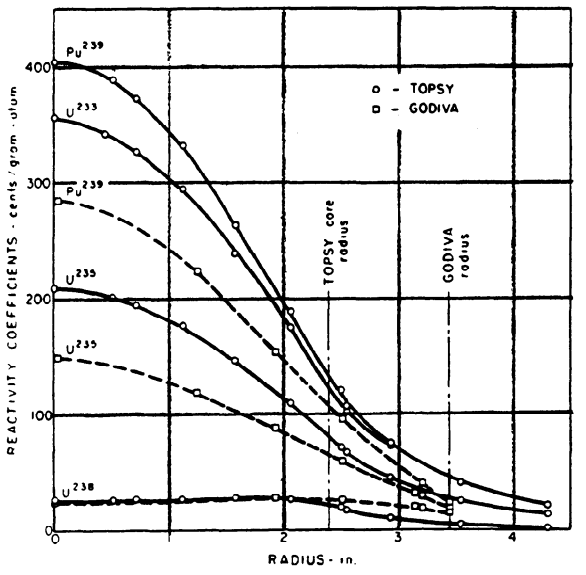

FIG. 1. Reactivity coefficients for fissionable materials in Topsy (U reflector) and Godiva.

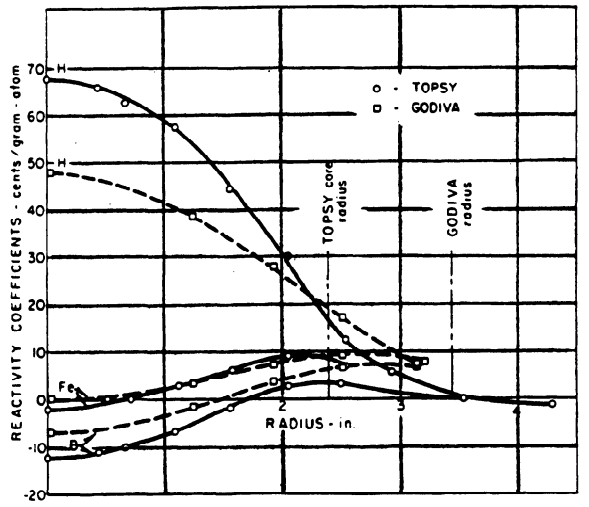

FIG. 2. Illustrative reactivity coefficients for nonfissionable materials in Topsy (U reflector) and Godiva.

Figs. 3 and 4. The shapes of these functions are determined by the radial dependences of $\Delta k_0(r, x)$ with a pure absorber and pure scatterer, respectively. The former is represented by combinations such as $\Delta k_0(r, \text{Pu}) - \Delta k_0(r, \text{Oy})$ or $\Delta k_0(r, \text{Oy}) - \Delta k_0(r, \text{U})$ since $\sigma_{tr}(\text{Pu}) \simeq \sigma_{tr}(\text{Oy}) \simeq \sigma_{tr}(\text{U})$, while the latter may be represented by elements such as Al where $\sigma_a \simeq 0$. The relative values of $f_0(r)$ and $f_1(r)$ are fixed by requiring agreement with Eq. (II-2) at small values of r, and the absolute values then determined by the above-mentioned choice of the constant c.

For a majority of elements, $\Delta k_0(r, x)$ has a maximum value in the vicinity of $r \sim 2$ in. (for Oy cores), and the value of $\sigma_{tr}(x)$ is determined mainly by the Δk measurements in the range 1.5–2.5 in. Typically, in this range, $\Delta k \sim 10$ cents/g-atom with an experimental precision of ~0.2–0.3 cents/g-atom, so that the apparent transport cross section $\sigma_{tr}(x)$ can be specified with a relative precision of 2–3%. The exceptions are (i) U in Topsy (through influence on σ_a of large spectral changes near the core surface); (ii) the highly fissionable materials Pu, U^{233}, and Oy [because a universal function $f_1(r)$ cannot permit sufficiently accurate subtraction of the very large absorptive component, $-\sigma_a(x)f_0(r)$ from $\Delta k_0(r, x)$]; and (iii) hydrogen and deuterium (because of a change with radius of the energy dependence of the adjoint or neutron effectiveness).

Included in the tables of reactivity coefficients, $\Delta k_0(r, x)$ (Tables VI and VII) for the Topsy U and Topsy Ni assemblies, is the additional column $\Delta k_0(r = 0, x)$. The normal stacking of the Topsy assemblies prevented access to the core centers, and the values in this additional column are obtained from $\Delta k_0(r = 0, x) \equiv -\sigma_a(x)f_0(r = 0)$. It may be noted that for the weakly absorbing materials, there is a large percentage difference between $\Delta k_0(r = 0, x)$ and the nearest observed value $\Delta k_0(r \sim 0.5 \text{ in.}, x)$. The difference is due almost entirely to the scattering contribution to reactivity change at the $r \sim 0.5$ in. sample position. Since $\sigma_{tr}(x)$ values are accurately determined in the same experiment, the extrapolation to $\Delta k_0(r = 0, x)$ is unambiguous.

The detailed significance of σ_{tr}, and the breakdown of σ_a into components arising from capture (and fission) and from energy degradation by scattering are discussed by Hansen and Maier (*6*). The scattering contribution to σ_a is evaluated by Byers (*7*) in cases where appropriate capture cross sections have been measured and his results are used in Section IV.

III. CRITICAL MASSES OF MILDLY DILUTED U^{235} AND Pu^{239} SYSTEMS DERIVED FROM REACTIVITY COEFFICIENTS

The relationship for critical mass versus concentration of a diluent is obtained as follows for Topsy, Godiva, and Jezebel. Let the reactivity coefficient (per gram atom) of enriched uranium or plutonium at a given radius (r) be $\Delta k(r, \text{Oy or Pu})$. The reactivity contribution per unit volume is then

$$\Delta k(r, \text{Oy or Pu})\rho/A,$$

where ρ is the density and A is the average atomic mass of the uranium or plutonium. Similarly, the reactivity contribution per unit volume for an ele-

TABLE X

Apparent Absorption and Transport Cross Sections

Element	σ_a (barns)				σ_{tr} (barns)			
	Topsy-U	Topsy-Ni	Godiva	Jezebel	Topsy-U	Topsy-Ni	Godiva	Jezebel
H	-0.610		-0.599[a]	-0.141				1.18
D	-0.216		-0.223[a]	0.013				1.88
Li^6	0.597							
Li^7	-0.035							
Be	-0.083		-0.093	-0.036	1.82		2.17	2.25
B^{10}		0.790	0.721	0.56_1			2.62	1.90
B	0.110	0.103	0.088				2.10	
C	-0.022	-0.023	-0.028[a]	0.016	2.13	2.20	2.17	2.15
N				0.05				1.7_2
O	-0.013		-0.012[b]	0.023	2.20			2.22
F	-0.04		-0.054[b]	0.04_1	2.30			2.7_2
Mg	-0.013				2.37			
Al	-0.006	-0.008	-0.006[a]	0.032	2.12	2.17	2.14	2.30
Si				0.039				2.34
S	0.080			0.15_9	2.04			1.60
Ca	0.06				1.94			
Ti	0.017	-0.001		0.054	2.16	2.29		2.48
V	0.000		-0.012[b]	0.033	2.90			2.7_2
Cr	0.015				2.41			
Mn	0.009		-0.017[b]		2.70			
Fe	0.020	0.013	0.006	0.049	2.29	2.53	2.29	2.44
Co	0.023		0.007[a]	0.057	2.73		2.75	2.76
Ni	0.066	0.056	0.056[a]	0.109	2.77	2.36	2.65	2.77
Cu	0.035	0.025	0.022[a]	0.073	2.68	2.85	2.73	2.83
Zn	0.047		0.030	0.092	2.86		2.78	2.85
Ga	0.036	0.009	0.012[b]		2.87	3.02		
As	0.018		-0.003[b]		3.91			
Zr	0.022			0.07	3.87			4.1
Nb	0.068		0.021[b]		3.99			
Mo	0.032			0.103	4.58 (?)			3.99
Rh	0.127		0.095[b]		3.38			
Pd	0.093				3.51			
Ag	0.162		0.127[a]	0.209	3.26		3.55	3.54
Cd	0.086			0.146	3.51			3.65
In	0.233			0.183[b]	3.33			
Sn	0.040			0.100	3.31			3.49
Sb	0.131		0.080[b]		3.31			
I	0.122		0.076[b]		3.55			
La	0.016		0.021[b]	0.08_2	3.47			3.1_6
Ce	0.041			0.07_6	3.54			3.6_7
Nd	0.078				3.41			
Dy			0.20					
Ho			0.35					4.2
Yb			0.18					
Ta	0.155		0.112	0.228	3.91			4.34

TABLE X (*Continued*)

Apparent Absorption and Transport Cross Sections

Element	σ_a (barns)				σ_{tr} (barns)			
	Topsy-U	Topsy-Ni	Godiva	Jezebel	Topsy-U	Topsy-Ni	Godiva	Jezebel
W	0.097		0.050	0.179	4.40			4.60
Pt	0.097				4.34			
Au	0.143	0.093	0.093[a]	0.196	4.17	4.11	4.43	4.48
Pb	0.014		0.009[b]		4.26			
Bi	0.037	0.015	0.021[a]	0.053	4.64	4.32	4.60	4.62
Th	0.069	0.017	0.017	0.139	4.48	4.64	4.92	5.00
U^{233}	-3.258	-3.147		-3.07				
U^{235}	-1.893[d]	-1.887[d]	-1.860[d]	-1.81_8				5.3[e]
U^{238}	-0.243	-0.271	-0.303	-0.258	5.1[d]	5.1[d]	5.0[d]	5.1[de]
Np^{237}	-1.59			-1.78				
Pu^{239}	-3.657	-3.602	-3.553	-3.600[d]				5.3[e]
Pu^{240}	-2.60[c]		-2.1	-2.35				

[a] Compare with σ_a from large-sample measurements (Section IV).

[b] From large-sample measurements of Section IV.

[c] Though this value arises from measurements on Pu samples with various Pu^{240} contents, showing apparent consistency of ± 4%, it disagrees seriously with expectations from Godiva and Jezebel measurements.

[d] Normalized to these values.

[e] Compare with values of σ_{tr} from the appendix.

ment (x) is $\Delta k(r, x)\rho''/A''$, where ρ'' is the density and A'' is the atomic mass of element (x). When the volume fraction of enriched uranium or plutonium is changed by ΔF as the result of substituting the element (x), a reactivity change occurs which can be expressed as the sum of all reactivity changes occurring in each core volume element due to the change $\Delta F/F$. The reactivity change obtained by replacing core material by the diluent (x) throughout the core volume is then

$$\Delta k_1 = 4\pi \frac{\Delta F}{F}\left[\int_0^{r_0} \Delta k(r, \text{Oy or Pu}) \frac{\rho}{A} r^2\, dr - \int_0^{r_0} \Delta k(r, x) \frac{\rho''}{A''} r^2\, dr\right] \tag{III-1}$$

When the core volume for the Topsy assembly (enriched uranium core with normal uranium reflector) is changed by ΔV_c through the interchange of enriched uranium and normal uranium at the core surface, a reactivity change results which is defined as Δk_2. With U (normal) of density ρ' and atomic mass A', the reactivity change per mole at the core-reflector interface is $\Delta k(r_0, U)$ and for enriched uranium is $\Delta k(r_0, \text{Oy})$. Δk_2 is then

$$\Delta k_2 = \Delta V_c\left[\Delta k(r_0, \text{Oy}) \frac{\rho}{A} - \Delta k(r_0, U) \frac{\rho'}{A'}\right] \tag{III-2}$$

For the system to remain at delayed critical,

$$\Delta k_1 + \Delta k_2 = 0 \tag{III-3}$$

Combining Eqs. (III-1), (III-2), and (III-3), and noting that the fractional change in critical mass of enriched uranium is

$$\frac{\Delta m_c}{m_c} \cong \frac{\Delta F}{F} + 3\frac{\Delta r_0}{r_0} \tag{III-4}$$

where $\Delta r_0 = \Delta R_0$ (R_0 being the reflector-air radius), and $A = A'$ for the normal assembly, one obtains for Topsy

$$\frac{\Delta m_c}{m_c} \cong \frac{\Delta F}{F} \left\{1 - \frac{3\left[\int_0^{r_0} \Delta k(r, \text{Oy})\, r^2 dr - \int_0^{r_0} \Delta k(r, x) \frac{\rho'' A}{\rho A''} r^2\, dr\right]}{r_0^3[\Delta k(r_0, \text{Oy}) - \Delta k(r_0, U)]}\right\} \tag{III-5}$$

For the Godiva or Jezebel assemblies (bare enriched uranium or plutonium) Δk_2 is simply

$$\Delta k_2 = \Delta V_c\left[\Delta k(r, \text{Oy or Pu}) \frac{\rho}{A}\right] \tag{III-6}$$

and one obtains the expression

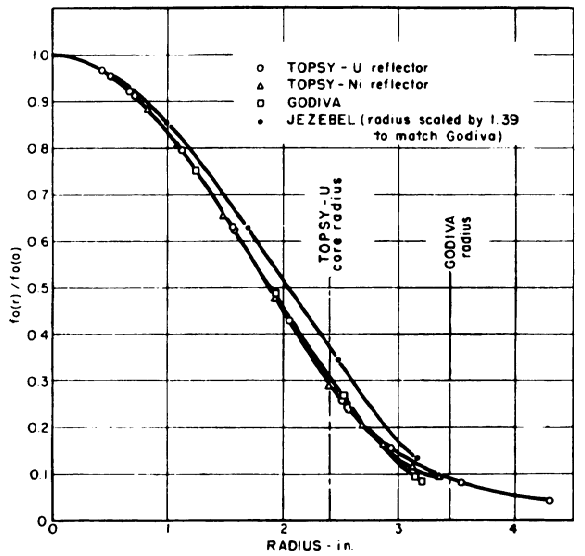

FIG. 3. $f_0(r)/f_0(0)$ vs radius for Topsy, Godiva, and Jezebel assemblies. $f_0(0)$ = 110.7 for Topsy with U reflector, 118 for Topsy with Ni reflector, 79.8 for Godiva, and 436 for Jezebel. The Topsy–Ni core radius is 2.55 in.

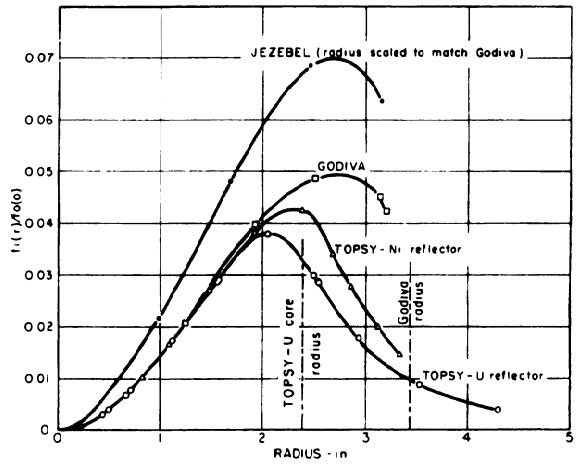

FIG. 4. $f_1(r)/f_0(0)$ for Topsy, Godiva, and Jezebel assemblies. $f_0(0)$ = 110.7 for Topsy with U reflector, 118 for Topsy with Ni reflector, 79.8 for Godiva, and 436 for Jezebel. The Topsy-Ni core radius is 2.55 in.

$$\frac{\Delta m_c}{m_c} \cong \frac{\Delta F}{F} \cdot \left\{ 1 - \frac{3\left[\int_0^{r_0} \Delta k(r, \text{Oy or Pu})\, r^2 dr - \int_0^{r_0} \Delta k(r, x)\, \frac{\rho'' A}{\rho A''}\, r^2\, dr\right]}{r_0^3[\Delta k(r_0, \text{Oy or Pu})]} \right\} \quad \text{(III-7)}$$

It has been shown that $\Delta k(r, x)$ can be represented by the expression,

$$\Delta k(r, x) = -\sigma_a(x) f_0(r) + \sigma_{tr}(x) f_1(r) \quad \text{(III-8)}$$

where $f_0(r)$ and $f_1(r)$ are functions of the radius alone for any given assembly, and $\sigma_a(x)$ and $\sigma_{tr}(x)$ are the effective absorption and transport cross sections of an element (x). When Eq. (III-8) is substituted into Eqs. (III-6) and (III-7), and results of graphical integrations of

$$\Delta k(r, \text{Oy or Pu}) r^2\, dr, \qquad f_0(r) r^2\, dr,$$

and $f_1(r) r^2\, dr$ are inserted, the following expressions are obtained:

For Topsy,

$$n_T = 1.20 - \frac{\rho''}{A''}[0.735\, \sigma_{tr}(x, T) - 12.82\, \sigma_a(x, T)] \quad \text{(III-9)}$$

for Godiva,

$$n_G = 2.00 - \frac{\rho''}{A''}[2.25\, \sigma_{tr}(x, G) - 14.27\, \sigma_a(x, G)] \quad \text{(III-10)}$$

and for Jezebel,

$$n_J = 2.00 - \frac{\rho''}{A''}[1.846\, \sigma_{tr}(x, J) - 9.96\, \sigma_a(x, J)] \quad \text{(III-11)}$$

where the exponent (n) is defined by

$$\frac{\Delta m_c}{m_c} \cong -n \frac{\Delta F}{F}, \text{ or } m_c = \text{const } F^{-n}$$

Again, F is the volume fraction of enriched uranium or plutonium within the core.

Values for the exponent (n) for the Topsy and Godiva assemblies are given in Table XI and for Jezebel in Table XII. These values were obtained by using the above expressions with the listed effective cross section data for the different elements for which replacement data exist. Densities for the different elements are maximum values from the Metals Handbook. Effective cross sections for Zeus and Zephyr[2] are included in the tables to indicate sensitivity to dilution (8).

The tabulated exponent n = 1.20 for density change of the Topsy core was confirmed by gross

[2] Dr. R. D. Smith of Harwell has kindly provided these cross sections. Zeus and Zephyr consisted of rods packed to form hexagonal-cylindric cores surrounded by thick reflectors primarily of natural uranium. The Zeus (No. 1) core averaged about 49 v/o (volume per cent) Oy (25.5), 6 v/o Nb, 2.5 v/o Ni, 12 v/o Al, and 30.5 v/o void. The Zephyr (No. 1) core is estimated to be 50 v/o δ-phase Pu, 33 v/o U, 10 v/o Ni (with a small quantity of Cu), and 7 v/o void.

density changes that extended to 50% of normal density. Similarly, gross dilution by natural uranium (to one-half volume fraction) gave 0.73 for the U^{238} dilution exponent, which compares with 0.74 from Table XI.

IV. LARGE-CAVITY MEASUREMENTS AT GODIVA CENTER

Central Godiva Values as Function of Z

A second group of measurements on Godiva was designed to give more detail about effective absorp-

TABLE XI

Dilution Exponents for Topsy and Godiva with Comparative Cross Sections for Zeus

Element (x)	Density g-atom/cm^3	Topsy (Oy 94% in U)			Godiva (bare Oy 94%)			Zeus (No. 1)[a]	
		$\sigma_a(x)$ barn	$\sigma_{tr}(x)$ barn	Dilution exponent n(x)	$\sigma_a(x)$ barn	$\sigma_{tr}(x)$ barn	Dilution exponent n(x)	$\sigma_a(x)$ barn	$\sigma_{tr}(x)$ barn
H		-0.610			-0.599			-0.220	1.2
D		-0.216			-0.223			-0.065	0.8
Li	0.077	0.015			0.016[b]				
Li^6	0.077	0.597						0.74	
Be	0.202	-0.083	1.82	0.72	-0.093	2.17	0.75	-0.032	2.4
B	0.212	0.110			0.088	2.10	1.26	0.155	1.9
B^{10}	0.212				0.721	2.62		1.040	
C	0.185	-0.022	2.13	0.86	-0.028	2.17	1.02	-0.013	2.8
O		-0.013	2.20		-0.012[b]			-0.010	3.2
F		-0.04	2.30		-0.054[b]			-0.022	2.8
Na					-0.014[b]			-0.003	3.5
Mg	0.072	-0.013	2.37	1.06				-0.002	3.4
Al	0.100	-0.006	2.12	1.04	-0.006	2.14	1.51	0.010	3.2
Si	0.083							-0.001	3.0
P					0.018[b]				
S	0.064_5	-0.080	2.04	1.15					
Cl					0.057[b]				
K					0.039[b]			0.034	2.3
Ca	0.039	0.060	2.16	1.16					
Sc					-0.008[b]				
Ti	0.095	0.017	2.16	1.03				0.019	3.2
V	0.118	0.000	2.90	0.95	-0.012[b]			0.010	4.0
Cr	0.138	0.015	2.41	0.98				0.020	
Mn	0.135	0.009	2.70	0.95	-0.017[b]			0.012	3.4
Fe	0.137	0.020	2.29	1.01	0.006	2.29	1.28	0.022	2.9
Co	0.151	0.023	2.73	0.94	0.007	2.75	1.08	0.031	3.9
Ni	0.152	0.066	2.77	1.02	0.056	2.65	1.22	0.040	3.5
Cu	0.141	0.035	2.68	0.99	0.022	2.73	1.18	0.037	3.7
Zn	0.109	0.047	2.86	1.04	0.030	2.78	1.36	0.043	4.2
Ga	0.085	0.036	2.87	1.06	0.012[b]				
As	0.076	0.018	3.91	1.00	-0.003[b]				
Se								0.053	5.2
Br					0.020[b]			0.124	4.3
Rb					0.019[b]				
Y					-0.011[b]				
Zr	0.071	0.022	3.87	1.02				0.029	5.7
Nb	0.092	0.068	3.99	1.01	0.021[b]			0.092	5.0
Mo	0.106	0.032	4.58(?)	0.89				0.068	5.1
Rh	0.121	0.127	3.38	1.10	0.095[b]				
Pd	0.113	0.093	3.51	1.04					
Ag	0.097	0.162	3.26	1.17	0.127	3.55	1.40	0.268	4.5
Cd	0.077	0.086	3.51	1.09				0.122	4.9

TABLE XI (*Continued*)

Dilution Exponents for Topsy and Godiva with Comparative Cross Sections for Zeus

Element (x)	Density g-atom/cm^3	Topsy (Oy 94% in U)			Godiva (bare Oy 94%)			Zeus (No. 1)[a]	
		$\sigma_a(x)$ barn	$\sigma_{tr}(x)$ barn	Dilution exponent n(x)	$\sigma_a(x)$ barn	$\sigma_{tr}(x)$ barn	Dilution exponent n(x)	$\sigma_a(x)$ barn	$\sigma_{tr}(x)$ barn
In	0.064	0.233	3.33	1.24	0.183[b]			0.279	5.1
Sn	0.061_5	0.040	3.31	1.08				0.063	4.7
Sb	0.054_5	0.131	3.31	1.16	0.080[b]			0.184	5.0
Te								0.066	4.5
I	0.039	0.122	3.55	1.16	0.076[b]			0.200	4.4
Cs					0.083[b]				
Ba								0.042	
La	0.044	0.016	3.47	1.10	0.021[b]				
Ce	0.049	0.041	3.54	1.10					
Pr					0.017[b]				
Nd	0.049	0.078	3.41	1.13					
Ta	0.092	0.155	3.91	1.12	0.112[b]			0.250	5.4
W	0.105	0.097	4.40	0.99	0.050			0.117	4.7
Re					0.162[b]				
Ir					0.120[b]				
Pt	0.110	0.097	4.34	0.98					
Au	0.098	0.143	4.17	1.08	0.093	4.43	1.16	0.200	5.5
Hg								0.079	
Tl					0.010[b]				
Pb	0.055	0.014	4.26	1.04	0.009[b]			0.025	6.3
Bi	0.047	0.037	4.64	1.06	0.021	4.60	1.53	0.026	6.7
Th	0.049_5	0.069	4.48	1.08	0.017	4.92	1.46	0.133	6.7
U	0.080	-0.242		0.73[c]	-0.310		0.74	0.018	5.8
U^{233}	0.080	-3.220						-3.380	
U^{235}	0.080	-1.893[c]			-1.860[d]	5.1[e]		-1.890	10.9
U^{238}	0.080	-0.228	5.10[d]	0.74[cf]	-0.299	5.0[d]	0.76	0.032	
Np^{237}		-1.40							
Pu^{239}		-3.636			-3.561	5.2[e]		-3.380	
Pu^{240}		-2.58(?)			-2.1				
Void				1.20[cg]			2.00		

[a] Information kindly provided by Dr. R. D. Smith of Harwell.

[b] From large-sample measurements of Section IV.

[c] Integrated separately.

[d] Used for normalization.

[e] From appendix.

[f] Compares with 0.73 observed directly from Oy(47) to Oy(94).

[g] Compares with 1.20 observed directly from 50% to 100% normal density.

tion cross sections, particularly the apparent periodicity against Z for the isotopically simple odd Z – odd A elements (a few other elements were included). As the emphasis was on reliable relative values rather than minimum perturbation of Godiva, large samples were used. Each material was sealed in a cylindrical Al can of $\frac{3}{4} \times \frac{3}{4}$ in. inside dimensions, which fit into a $\frac{15}{16} \times \frac{15}{16}$ in. cylindrical cavity at the center of Godiva. Reactivity contributions were determined relative to the system with an empty Al can in the cavity. The results of these measurements, with estimated probable errors, are listed in Table XIII. The material in each sample also is described. At least two determinations were made with each sample, and where the presence of moisture was suspected, measurements were repeated in the course of progressive drying until a stable condition was attained.

The central reactivity contributions of odd Z – odd A elements are shown in Fig. 5 as a function of Z.

The pattern corresponds in general to similar data reported for the Los Alamos fast reactor (*9*), Clementine, and for Harwell's Zeus and Zephyr (*8*). In view of the behavior of capture cross sections for fission neutrons, reported by Hughes *et al.* (*10*) it is not surprising that there is strong suggestion of a magic number influence on reactivity contributions by this isotopically simple class of elements.

TABLE XII

Dilution Exponents for Jezebel with Comparative Cross Sections for Zephyr

Element (x)	Density g-atom/cm^3	Jezebel (bare Pu) $\sigma_a(x)$ barn	Jezebel (bare Pu) $\sigma_{tr}(x)$ barn	Jezebel (bare Pu) Dilution exponent n(x)	Zephyr (No. 1)[a] $\sigma_a(x)$ barn	Zephyr (No. 1)[a] $\sigma_{tr}(x)$ barn
H		-0.141	1.18		-0.189	
D		0.013	1.88		-0.029	
Li					0.032	0.9
Li^6					0.786	
Be	0.202	-0.037	2.25	1.09	-0.031	2.0
B					0.165	2.0
B^{10}		0.561	1.90		0.786	
C	0.185	0.016	2.15	1.30	0	2.4
N		0.05	1.72		0.080	1.8
O		0.023	2.22		0	2.5
F		0.04_1	2.72		0.002	2.8
Na					0.021	2.9
Mg					0.014	2.6
Al	0.100	0.033	2.30	1.61	0.026	2.7
Si	0.083	0.040	2.34	1.68	0.022	2.5
P					0.061	2.5
S	0.064_5	0.161	1.60	1.91	0.085	2.2
Cl					0.067	2.2
K					0.059	2.5
Ca					0.076	2.5
Sc					0.040	2.2
Ti	0.095	0.055	2.48	1.62	0.031	2.6
V	0.118	0.034	2.72	1.45	0.034	3.2
Cr					0.035	2.6
Mn					0.023	2.8
Fe	0.137	0.050	2.44	1.45	0.055	2.9
Co	0.151	0.058	2.76	1.32	0.051	3.0
Ni	0.152	0.111	2.77	1.39	0.093	3.2
Cu	0.141	0.074	2.83	1.37	0.074	3.2
Zn	0.109	0.093	2.85	1.53	0.083	3.3
Ga					0.081	3.3
Ge					0.077	3.4
As					0.114	4.1
Se					0.088	4.1
Br					0.148	3.4
Rb					0.073	3.3
Sr					0.061	4.9
Y					0.045	5.9
Zr	0.071	0.070	4.10	1.51	0.040	4.6
Nb					0.141	4.9
Mo	0.106	0.105	3.99	1.33	0.105	4.4
Ru					0.126	3.6
Rh					0.217	

TABLE XII (*Continued*)

Dilution Exponents for Jezebel with Comparative Cross Sections for Zephyr

Element (x)	Density g-atom/cm^3	Jezebel (bare Pu) $\sigma_a(x)$ barn	Jezebel (bare Pu) $\sigma_{tr}(x)$ barn	Jezebel (bare Pu) Dilution exponent n(x)	Zephyr (No. 1)[a] $\sigma_a(x)$ barn	Zephyr (No. 1)[a] $\sigma_{tr}(x)$ barn
Pd					0.165	4.1
Ag	0.097	0.212	3.54	1.57	0.250	3.7
Cd	0.077	0.148	3.65	1.60	0.156	4.1
In					0.305	4.1
Sn	0.061_5	0.102	3.49	1.67	0.102	4.0
Sb					0.171	3.6
Te					0.114	4.4
I					0.238	3.5
Cs					0.215	3.2
Ba					0.075	5.0
La	0.044	0.083	3.16	1.78	0.090	
Ce	0.049	0.077	3.67	1.71	0.069	
Eu					0.330	5.2
Hf					0.177	4.7
Dy		0.20				
Ho		0.35	4.2			
Yb		0.18				
Ta	0.092	0.232	4.34	1.48	0.265	4.3
W	0.105	0.182	4.60	1.30	0.174	4.9
Re					0.310	3.6
Os					0.146	4.1
Ir					0.303	4.4
Pt					0.178	4.8
Au	0.098	0.199	4.48	1.38	0.220	4.7
Hg					0.120	4.9
Tl					0.095	5.6
Pb					0.060	5.1
Bi	0.047	0.054	4.62	1.62	0.046	5.1
Th	0.049_5	0.141	5.00	1.66	-0.169	5.8
U	0.080	-0.249	5.1	1.05	-0.124	5.1
U^{233}	0.080	-2.88			-3.32	6.5
U^{235}	0.080	-1.828	5.3		-1.850	6.1
U^{238}	0.080	-0.238	5.1[b]	1.06		
Np^{237}		-1.52				
Pu^{239}		-3.600[b]	5.3		-3.660	4.8
Pu^{240}		-2.34				
Void				2.00		

[a] Information kindly provided by Dr. R. D. Smith of Harwell.

[b] Used for normalization.

Maxima (or plateaus in generally rising regions) appear in the neighborhood of Z = 20, 50 and 82 (or 80) and N = 20, 50, 82, and 126.

Capture and Scattering Components

A central reactivity contribution may, in principle, be separated into a capture effect and scattering effect. Capture, of course, gives a negative contribution, but in an assembly such as Godiva, energy degradation by scattering is expected to reduce the probability that neutrons escape fission thus increasing the reactivity (*11*).

For some elements of the class being considered, capture cross sections (σ_c) for the Godiva central

TABLE XIII

Godiva. Reactivity Contributions of Large Central Samples

Element	Z	Contribution, cents/g-atom	Sample wt - g	Remarks
H	1	+41.2 ± 0.5	see CH_2	
D	1	+14.9 ± 0.2	see D_2O	
Li	3	-1.04 ± 0.05	3.00	c.p. (Fisher), massive
C	6	+1.80 ± 0.07	3.23, 1.627	diamond, crystals
O	8	+0.8 ± 0.2	see Al_2O_3, PbO	
F	9	+3.6 ± 0.1	see C_2F_3Cl, NaCl	
Na	11	+0.9 ± 0.1	5.02	An. Reag. (Baker), massive
Al	13	+0.35 ± 0.06	9.75	(Baker), granular
P	15	-1.2 ± 0.1	7.05	yellow purified (Baker), massive
Cl	17	-3.8 ± 0.1	see CCl_4, NaCl, $PbCl_2$	
K	19	-2.6 ± 0.15	5.02	(Baker), massive
Sc	21	+0.5 ± 0.4	see Sc_2O_3	
V	23	+0.80 ± 0.08	12.48	99.7% (Mackay), massive
Mn	25	+1.10 ± 0.06	19.47	96%, C-free (Baker), massive
Co	27	-0.58 ± 0.06	18.70	98 - 100% (Baker), massive
Ni	28	-3.53 ± 0.04	28.34	c.p. An. low Co (Baker), shot
Cu	29	-1.14 ± 0.07	32.73	An. Reag. (Mallin.), shot
Ga	31	-0.80 ± 0.08	16.12	(from Rendell), massive
As	33	+0.2 ± 0.1	14.07	pure (Mallin.), granular
Br	35	-1.35 ± 0.25	see NaBr	
Rb	37	-1.25 ± 0.5	see RbBr	
Y	39	+0.7 ± 0.4	see Y_2O_3	
Nb	41	-1.4 ± 0.2	29.15	st'd grade (Fansteel), vac. dried
Rh	45	-6.25 ± 0.2	9.91	(Baker and Co.), powder, can not full
Ag	47	-8.1 ± 0.2	8.73	clean scrap
In	49	-12.1 ± 0.1	23.07	99.97% (In. Corp. of Am.), shot
Sb	51	-5.3 ± 0.1	22.74	c.p. (City Chem.), massive
I	53	-5.05 ± 0.2	12.74	An. Reag. (Mallin.), flake
Cs	55	-5.5 ± 0.3	see CsCl	
La	57	-1.4 ± 0.2	11.84	(Ames material, from Holley), massive
Pr	59	-1.1 ± 0.3	see Pr_2O_3	
Ta	73	-7.40 ± 0.08	53.92	(from Linenberger), 50 mesh
Re	75	-10.7 ± 0.3	20.07	99.9% (Varlacoid), vac. dried
Ir	77	-7.9 ± 0.9	see IrO_2	
Au	79	-5.6 ± 0.2	22.20	clean scrap
Tl	81	-0.66 ± 0.15	27.75	c.p. (Fisher), massive
Pb	82	-0.61 ± 0.10	41.18	c.p. (Braun), granular
Bi	83	-0.9 ± 0.15	35.32	c.p. An. (Baker), granular

Compound	Contribution, cents/mole	Sample wt - g	Remarks
CH_2	+84.1 ± 0.8	2.698	polythene, corr. from special geom.
D_2O	+30.48 ± 0.10	6.602	99.8%
Al_2O_3	+2.8 ± 0.2	5.99	An. Reag. (Baker), heat dried
PbO	+0.3 ± 0.2	22.89	An. Reag. (Mallin.), heat dried
NaF	+4.6 ± 0.1	7.38	c.p. An. (Baker), heat dried
C_2F_3Cl	+10.5 ± 0.2	11.75	fluorothene G
CCl_4	-13.35 ± 0.40	8.84	An. Reag. (Mallin.)
NaCl	-2.9 ± 0.15	6.73	An. Reag. (Mallin.), heat dried
$PbCl_2$	-6.8 ± 0.4	16.57	Reag. (Merck), undried powder
Sc_2O_3	+3.4 ± 0.6	4.29	Spec. An. (Pfaltz and Bauer), heat dried
NaBr	-0.45 ± 0.2	8.14	An. Reag. (Mallin.), heat dried
RbBr	-2.6 ± 0.5	5.19	c.p. (Fisher), heat dried
Y_2O_3	+3.8 ± 0.6	6.95	99% (Res. Chem., Inc.), heat dried
CsCl	-9.3 ± 0.3	9.65	c.p. (Fisher), heat dried
Pr_2O_3	+0.2 ± 0.4	10.21	98% (Res. Chem., Inc.), heat dried
IrO_2	-6.3 ± 0.8	10.02	(Baker and Co.), heat dried

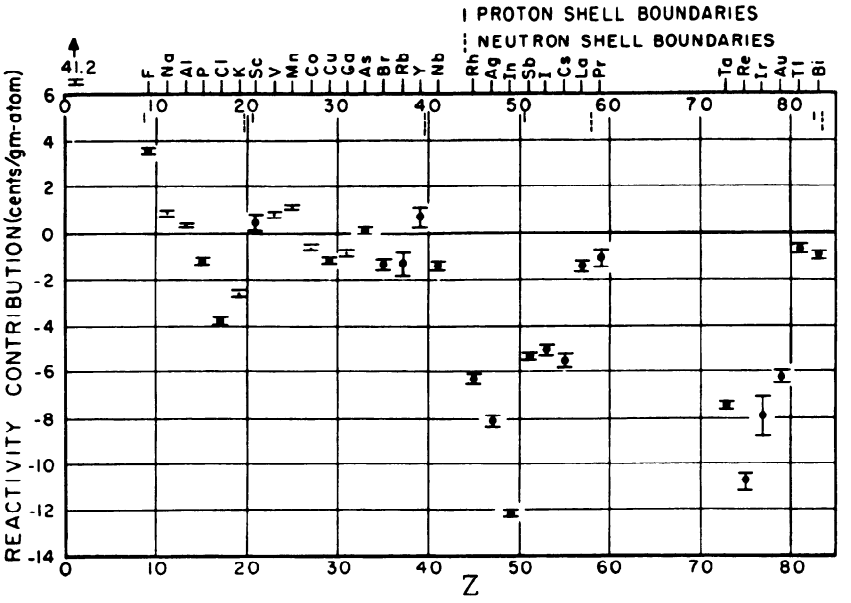

FIG. 5. Godiva central reactivity coefficients for odd Z – odd A elements.

spectrum have been measured by Byers (7) and others may be estimated from published data.

For comparison with σ_c, effective absorption cross sections may be obtained from reactivity contribution values by means of Eq. (II-1). For the central position, this relation may be rewritten

$$\sigma_a(x) = \sigma_a(\text{Oy})[\Delta k_0(x)/\Delta k_0(\text{Oy})]$$

where $\sigma_a(x)$ is the effective absorption cross section of nuclide x. As before, $\sigma_a(\text{Oy}) = 1.77$ barns, and by taking $\Delta k_0(\text{Oy}) = 117$ cents/mole, the value for a small Oy sample in a $\frac{15}{16} \times \frac{15}{16}$ in. cylindrical cavity, $\Delta k_0(x)$ for a nonfissionable (low absorption) material is simply the observed reactivity contribution. Table XIV lists σ_a, corresponding estimates of σ_c for Godiva, and the scattering residues, $\sigma_c - \sigma_a$.

Scattering Residues as Function of Z

The resulting estimates of inelastic scattering component for odd Z – odd A elements are shown vs Z in Fig. 6. Again a periodicity with Z is suggested, such that maximum inelastic scattering (at least in the two most pronounced cases) coincides with maximum absorption. Two cases of negative scattering residues fall at magic neutron numbers.

APPENDIX I: RELATIVE TRANSPORT CROSS SECTIONS OF Pu, Oy (93.5%), AND U IN GODIVA

The reactivity contributions of samples of Pu, Oy (93.5%), and U placed just beyond the Godiva surface were measured in an attempt to improve the information on the relative transport cross sections of these materials. (These heavy elements were known to have nearly equal transport cross sections). For such a sample position, the reactivity contribution is proportional to the number of neutrons sent back to the core (per core fission or other flux level unit) and is thus a measure of the cross section $\nu\sigma_f + \bar{\sigma}_s$. Although the highly anisotropic flux distribution beyond the Godiva surface gives rise to a complicated weighting of the angular distribution of elastically scattered neutrons, one expects $\bar{\sigma}_s$ to be comparable to the transport scattering cross section, and hence that $\bar{\sigma}_s + \sigma_f + \sigma_{n,\gamma} = \bar{\sigma}$ be comparable to the transport cross section.

Table XV lists the measured reactivity contributions for both the externally positioned samples and samples placed within but near the Godiva surface. It is seen that the ratio $\Delta k(\text{Pu})/\Delta k(\text{Oy})$ or the ratio $\Delta k(\text{Oy})/\Delta k(\text{U})$ varies with radial sample position, r, until the Godiva surface is reached, then remains constant at 1.37 ± 0.02. Because the self-multiplication of the Pu sample is the largest and that of the U sample the smallest, the limiting values of these experimental ratios exceed those of the reactivity coefficient or $\nu\sigma_f + \bar{\sigma}_s$ ratios. With the customary "size correction" on the experimental values, these latter ratios become

$$\frac{\{[(\nu-1)\sigma_f - \sigma_{n,\gamma}] + \bar{\sigma}\}_{\text{Pu}}}{\{[(\nu-1)\sigma_f - \sigma_{n,\gamma}] + \bar{\sigma}\}_{\text{Oy}}} = 1.28 \pm 0.02$$

$$\frac{\{[(\nu-1)\sigma_f - \sigma_{n,\gamma}] + \bar{\sigma}\}_{\text{Oy}}}{\{[(\nu-1)\sigma_f - \sigma_{n,\gamma}] + \bar{\sigma}\}_{\text{U}}} = 1.30 \pm 0.02$$

TABLE XIV

Interpretation of Material Replacement Data for Godiva Center

(Large Samples in 15/16 in. x 15/16 in. Cylindrical Cavity)

Element	Apparent absorption cross section (σ_a, barns)	σ_c (barns)	Scattering effect ($\sigma_c-\sigma_a$, barns)
H	-0.623 ± 0.008		
D	-0.225 ± 0.003		
Li	0.0157 ± 0.0009		
C	-0.0272 ± 0.0011		
O	-0.012 ± 0.003		
F	-0.054 ± 0.0015	0.0090[a]	0.063
Na	-0.014 ± 0.0015	(0.0014)[b]	(0.015)
Al	-0.0053 ± 0.0009	(0.0038)[b]	(0.009)
P	0.018 ± 0.0015		
Cl	0.057 ± 0.0015		
K	0.039 ± 0.002	< 0.004[c]	-0.035
Sc	-0.008 ± 0.006		
V	-0.0121 ± 0.0012	0.0029	0.015
Mn	-0.0166 ± 0.009	0.0033	0.020
Co	0.0088 ± 0.0009	~ 0.081	~ 0.077
Ni	0.0534 ± 0.0006		
Cu	0.0172 ± 0.0011	0.0127	-0.009
Ga	0.0121 ± 0.0012		
As	-0.0030 ± 0.0015	0.0562	0.059
Br	0.020 ± 0.004	0.0669	0.047
Rb	0.019 ± 0.008	~ 0.045	~ 0.026
Y	-0.011 ± 0.006	0.0086	0.020
Nb	0.021 ± 0.003	0.037	0.016
Rh	0.095 ± 0.003	0.164[a]	0.069
Ag	0.123 ± 0.003	0.194[a]	0.071
In	0.183 ± 0.0015	0.243[d]	0.060
Sb	0.080 ± 0.0015	0.120[d]	0.040
I	0.076 ± 0.003	0.104	0.028
Cs	0.083 ± 0.005		
La	0.021 ± 0.003	0.009	-0.012
Pr	0.017 ± 0.005	0.0165[a]	0.000
Ta	0.112 ± 0.0012	0.152	0.040
Re	0.162 ± 0.005	~ 0.198	~ 0.036
Ir	0.120 ± 0.014		
Au	0.085 ± 0.003	0.123	0.038
Tl	0.010 ± 0.002		
Pb	0.009 ± 0.0015		
Bi	0.014 ± 0.002	0.001	-0.013

[a] Fission-spectrum cross sections scaled by 1.5 (13).
[b] σ(n,α), σ(n,p) included, but not scaled by 1.5 (14).
[c] Measured by Hess of ANL (15).
[d] Estimated from σ_c vs neutron energy (16).

The ratios $\bar{\sigma}_{Pu}/\bar{\sigma}_{oy}$ and $\bar{\sigma}_U/\bar{\sigma}_{oy}$ are now determinable from the sample replacement measured values of $(\sigma_a)_{Pu}/(\sigma_a)_{oy}$ and $(\sigma_a)_U/(\sigma_a)_{oy}$ given in Table X together with one value of

$$[(\nu - 1)\sigma_f - \sigma_{n,\gamma}]/\bar{\sigma}.$$

We adopt $\{[(\nu - 1)\sigma_f - \sigma_{n,\gamma}]/\bar{\sigma}\}_{oy} = 0.34 \pm 0.01$ as the value of the excess number of neutrons produced per $\bar{\sigma}$ collision, this value being consistent

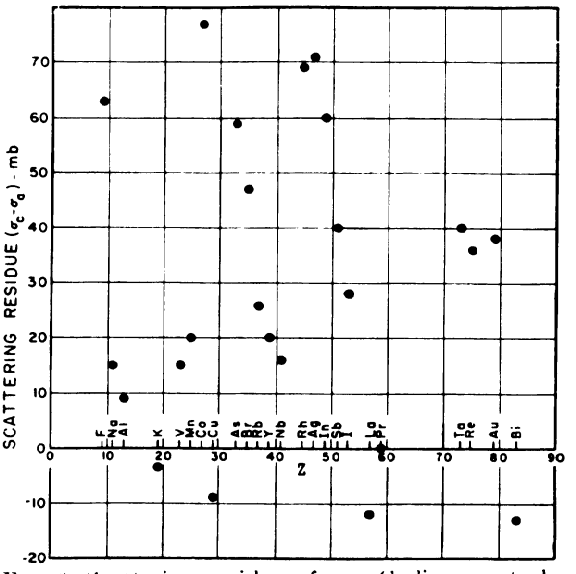

FIG. 6. Scattering residues from Godiva central reactivity coefficients for odd Z – odd A elements.

with cross-section measurements if $\bar{\sigma}$ is identified with the transport cross section. We then obtain[3]

$$\bar{\sigma}_{Pu}/\bar{\sigma}_{Oy} = 1.02 \pm 0.03$$

$$\bar{\sigma}_{U}/\bar{\sigma}_{Oy} = 0.98 \pm 0.02$$

APPENDIX II: CORRELATIONS BETWEEN REFLECTOR SAVINGS AND CROSS SECTIONS FROM REACTIVITY COEFFICIENTS

From critical masses of $5\frac{1}{4}$-in. diameter cylinders of Oy(93.5) in $\frac{1}{2}$ and 1-in. thick reflectors of various materials, corresponding reflector savings for spherical cores have been deduced (*12*). For a thin reflector of material x, the savings $(\Delta r)_x$ in cm Oy is proportional to $[Nt\sigma(1 + f)]_x$, where N is the nuclear density, t is the thickness, σ is the collision cross section (assumed to be the transport average), and f is the number of excess neutrons emitted per collision. In terms of the parameters for natural uranium, for which $\sigma(1 + f) = 5.4$ barns, then

$$[\sigma(1 + f)]_x = 5.4 \frac{(Nt)_U(\Delta r)_x}{(Nt)_x(\Delta r)_U} \text{ barns}$$

As $\sigma(1 + f)_x \simeq \sigma_{tr}(x) - \sigma_a(x)$, values deduced from the reflector savings measurements may be compared with corresponding values from reactivity coefficient data (Table X). The listing in Table XVI of both types of results show reasonable agreement except in the cases of Mo and the Topsy value for Be.

[3] Primarily because of the difference in the energy dependence of the neutron effectiveness at the center and surface of Godiva and the consequent difference in reactivity contributions due to inelastic scattering, we have used $\{[(\nu - 1)\sigma_f - \sigma_{n,\gamma}]_{Pu}/[(\nu - 1)\sigma_f - \sigma_{n,\gamma}]_{Oy}\}_{external} = (1.025 \pm 0.01)\ (\sigma_a)_{Pu}/(\sigma_a)_{Oy} = 1.025 \times 1.99 = 2.04 \pm 0.02$ and $\{[(\nu - 1)\sigma_f - \sigma_{n,\gamma}]_U/[(\nu - 1)\sigma_f - \sigma_{n,\gamma}]_{Oy}\}_{external} = (0.8 \pm 0.1)\ (\sigma_a)_U/(\sigma_a)_{Oy} = 0.8 \times 0.174 = 0.14 \pm 0.02$.

APPENDIX III. ESTIMATION OF THE AVERAGE NUMBER, ν, OF NEUTRONS PRODUCED PER FISSION FOR U^{233}, U^{235}, Pu^{239}, Pu^{240}, Np^{237}, AND U^{238}

The central Topsy, Godiva, and Jezebel reactivity coefficient data provide, for several of the fissionable isotopes, accurate values of the net neutron production cross section,

$$\sigma_p = [\nu - 1 - \alpha]\sigma_f .$$

Since the major neutron reaction parameters of most of these isotopes have already been measured as a function of neutron energy, the question arises as to what new information resides in the reactivity coefficient data. Especially for the threshold fissioners, the values of σ_p are sensitive to the neutron flux energy spectra of the critical assemblies, and in lieu of other flux sampling measurements, may best be utilized to characterize these spectra thereby indicating gross inelastic scattering properties of U^{235} and Pu^{239}. Combined with auxiliary measurements of σ_f, however, one obtains values for the much less spectral-sensitive quantity $[\nu - 1 - \alpha]$, and retains the spectral characterization of the critical assemblies. For the majority of $[\nu - 1 - \alpha]$ values so obtained, the probable uncertainties in available ν and α data imply $\Delta\nu > \Delta\alpha$; thus our present emphasis is on estimating ν.

Of major concern are the sources and magnitudes of the uncertainties accompanying each stage of this data reduction to ν values, not only to indicate the precision with which these values are determined but also to help establish what weak links may be clarified by reactivity coefficients when accurate results from measurements of $\nu(E)$ become available. Values of ν for various isotopes, deduced from the reactivity coefficient measurements in Topsy, Godiva, and Jezebel, have been reported elsewhere (*13–15*) and this provides another incentive for detailing the data reduction procedure.

A. THE RATIOS $\sigma_p(x)/\sigma_p(U^{235})$

Because of the energy dependence of the adjoint or neutron effectiveness functions, $\phi^+(E)$, characteristic of the critical assemblies, the measured reactivity coefficient ratios, $\Delta k_0(x)/\Delta k_0(U^{235})$, differ from the corresponding net neutron production

TABLE XV

Reactivity Contributions of Pu, Oy(93.5%), and U Samples Positioned near the Godiva Surface (r_c = 3.44 in.)

Radius (in.)	Δk(U) (¢/g-atom)	Δk(Oy) (¢/g-atom)	Δk(Pu) (¢/g-atom)	$\frac{\Delta k(Oy)}{\Delta k(U)}$	$\frac{\Delta k(Pu)}{\Delta k(Oy)}$
2.892	26.8	43.8	66.1	1.63	1.51
3.142	22.6	33.2	48.2	1.47	1.45
3.206	21.2	30.6	42.7	1.44	1.40
3.268[a]	19.3	27.4	--	1.42	--
3.285[a]	20.0	27.8	--	1.39	--
3.415[a]	17.3	24.4	--	1.41	--
3.456	12.8	18.4	25.9	1.44	1.41
3.541[a]	10.6 ± 0.1	14.6 ± 0.1	--	1.38 ± 0.02	--
3.706	7.8 ± 0.1	10.7 ± 0.1	14.7 ± 0.2	1.37 ± 0.02	1.37 ± 0.02

[a] At these radii, the U sample is a 50.3-g cylinder of length 0.295 in., outer diameter 0.875 in., and inner diameter 0.24 in.; the Oy sample is a 49.7-g cylinder of the same dimensions. At all other radii, the U sample is a 29.10-g solid cylinder of length 0.495 in. and diameter 0.495 in.; the Oy sample is a 30.08-g solid cylinder of length 0.500 in. and diameter 0.500 in.; the Pu sample is a 21.56-g solid cylinder of length 0.454 in. and diameter 0.488 in.

cross-section ratios, and one must compute, for each fissionable isotope, x, the quantity

$$C_x = [\sigma_p(x)/\sigma_p(U^{235})]/[\Delta k_0(x)/\Delta k_0(U^{235})]$$

according to the perturbation theory equation (IIIA-1) given below. In this equation $\phi(E)$ denotes the neutron flux, $\chi(E, E')$ denotes the normalized fission neutron spectrum for incident neutrons of energy E, $\sigma^{in}(E, E')$ denotes the differential inelastic scattering cross section, and for compactness the $n - 2n$ reaction is not included explicitly. Because $C_x \simeq 1$ is ensured by the weak energy dependence of $\phi^+(E)$; say $|\phi^+(E) - 1| \ll 1$, Eq. (IIIA-1) could be rephrased in terms of the small quantities $(C_x - 1)$ and $(\phi^+(E) - 1)$, thereby better illuminating the extent to which the poorly known neutron reaction cross sections of isotopes such as Np^{237} affect the precision of the computation of C_x. Rather than going into such detail, we shall assume a 50% uncertainty in our computed values of $(C_x - 1)$ for all x except U^{238}, and indicate only qualitatively the source of this uncertainty. For $x = Np^{237}$ or Pu^{240}, little or no data exist for $\sigma_{n,\gamma}(E)$ and $\sigma^{in}(E, E')$ and one is obliged to estimate these quantities from the empirical rule that the radiative capture cross sections of the heavy elements are equal, the nonelastic cross sections of the heavy elements are equal, and the spectrum of neutrons inelastically scattered from some primary energy by any heavy element is the same as that for U^{238}. It is felt that use of this empirical rule is the primary source of the 50% uncertainty ascribed to the computed $(C_x - 1)$ values for these isotopes.

For $x = U^{233}$ or Pu^{239}, the nuclear properties of x

$$C_x = \frac{\int dE\,[(\nu - 1 - \alpha)\sigma_f(E)]_x\,\phi(E)\phi^+(E)}{\int dE\,[(\nu - 1 - \alpha)\sigma_f(E)]_{U^{235}}\,\phi(E)\phi^+(E)} \cdot \frac{\int dE\,dE'[\nu\,\sigma_f(E)\chi(E, E') + \sigma^{in}(E, E')]_{U^{235}}\,\phi(E)\phi^+(E') - \int dE\,[(1 + \alpha)\sigma_f(E) + \sigma^{in}(E)]_{U^{235}}\,\phi(E)\phi^+(E)}{\int dE\,dE'[\nu\,\sigma_f(E)\chi(E, E') + \sigma^{in}(E, E')]_x\,\phi(E)\phi^+(E') - \int dE\,[(1 + \alpha)\sigma_f(E) + \sigma^{in}(E)]_x\,\phi(E)\phi^+(E)} \qquad \text{(IIIA-1)}$$

TABLE XVI

Correlation of Cross Sections from Reflector Savings and from Reactivity Coefficients

Reflector Material and density (g/cm^3)	Thickness (cm)	Reflector savings (cm Oy-93.5)	Reflector effect $\sigma(1+f)$ (barns)	$\sigma_{tr} - \sigma_a \equiv \sigma(1+f)$ (barns) Topsy	Godiva
Be (QMV)	2.54	1.45_9	2.32 ± 0.02[a]	1.92	2.30
1.84	1.27	0.89_6	2.30 ± 0.02[a]		
C (CS-312)	2.54	0.95_2	2.22 ± 0.02	2.18	2.34
1.67	1.27	0.59_7	2.25 ± 0.03	(2.23)[b]	
Mg (FS-1)	2.54	0.55_4	2.48 ± 0.05	2.41	--
1.77	1.27	0.37_8	2.73 ± 0.13		
Al (2S)	2.54	0.67_6	2.19 ± 0.02	2.16	2.19
2.70	1.27	0.43_3	2.27 ± 0.09	(2.19)[b]	
Ti (96.5 w/o)	2.54	0.64_6	2.23 ± 0.02	2.20	--
4.50	1.27	0.42_0	2.34 ± 0.10	(2.30)[b]	
Fe (SAE 1020)	2.54	0.91_8	2.14 ± 0.02	2.30	2.32
7.78 gm/cm^3	1.27	0.59_4	2.23 ± 0.03	(2.54)[b]	
Co (reagent)	2.54	1.19_6	2.63 ± 0.02	2.75	2.79
8.72	1.27	0.77_8	2.75 ± 0.02		
Ni (electrolytic)	2.54	1.15_9	2.52 ± 0.02	2.74	2.63
8.79	1.27	0.75_4	2.64 ± 0.02	(2.31)[b]	
Cu (99-99.5 w/o)	2.54	1.18_8	2.76 ± 0.02	2.67	2.76
8.87	1.27	0.75_2	2.82 ± 0.02	(2.83)[b]	
Mo (99.8 w/o)	2.54	1.21_9	3.61 ± 0.02	4.60	--
10.53	1.27	0.76_4	3.65 ± 0.02		
W (~91.3 w/o)	2.54	1.29_4	4.89 ± 0.03[c]	4.60[c]	--
17.3	1.27	0.81_6	4.97 ± 0.03[c]		
U (natural)	2.54	1.31_2	5.40[d]	5.40[d]	5.40[d]
18.8	1.27	0.81_4	5.40[d]	(5.40)[bd]	

[a] Effect of multiple scattering unknown.
[b] For Topsy with Ni reflector.
[c] For the "molecule" $W(Cu, Ni)_{0.093}$.
[d] Normalization value; $\sigma_{tr} - \sigma_a$ renormalized.

are similar to those of U^{235} and the small value of $C_x - 1$ depends significantly on such quantities as $(d\nu/dE)_x$ or $(d\nu/dE)_{U^{235}}$, not only through explicit appearance in Eq. (IIIA-1) but for U^{235} and Pu^{239}, implicitly in the functions $\phi^+(E)$. It is estimated that the sources of the 50% uncertainty in the computed $(C_x - 1)$ values for these isotopes are about evenly distributed between the nuclear description of x and the description of the characteristic functions, $\phi(E)$ and $\phi^+(E)$. For $x = U^{238}$, the value of $(C_x - 1)$ depends primarily on the accurately known (*16*) differential scattering cross section, and the estimated 20% uncertainty arises primarily in the uncertainties of $\phi^+(E)$. Table XVII lists the observed ratios $\Delta k_0(x)/\Delta k_0(U^{235})$ and the inferred ratios $\sigma_p(x)/\sigma_p(U^{235})$ from which our computed values of C_x may be inferred. Table XVIII lists the multigroup values of $\phi(E)$, $\phi^+(E)$, and several other quantities which play a significant role in the computation of C_x and subsequent computations. It may be noted in passing that the magnitude of uncertainty in $\phi^+(E)$ given above arises from the claimed precision in the measurements of the nuclear parameters of U^{235} and Pu^{239}. What few experimental checks on $\phi^+(E)$ that exist, such as the observed reactivity coefficients of hydrogen and deuterium, indicate smaller uncertainties in $\phi^+(E)$. (Unfortunately a good experimental check of the value $\phi^+ - 1$ does not exist for the highest energy group of Table XVIII, as this quantity is especially sensitive to $(d\nu/dE)$ of U^{235} in the case of Godiva or of Pu^{239} in the case of Jezebel.)

B. The Ratios $[\nu - 1 - \alpha]_x/[\nu - 1 - \alpha]_{U^{235}}$

The fission ratios

$$\sigma_f(U^{238})/\sigma_f(U^{235}) \quad \text{and} \quad \sigma_f(Np^{237})/\sigma_f(U^{235})$$

have been measured in the three critical assemblies and the results are listed in Table XVIII with corresponding computed values. Agreement between these computed and observed values is not fortuitous as the threshold detector data were utilized in the estimation of the inelastic transfer cross sections of Pu^{239} and U^{235} which, in turn, participate in the determination of $\phi(E)$ and $\phi^+(E)$. The main purpose for including the computed values is to indicate biases in $\phi(E)$ which affect the precision of the computed values of the spectrally insensitive ratios

$$\sigma_f(Pu^{240})/\sigma_f(Np^{237}), \quad \sigma_f(U^{233})/\sigma_f(U^{235}),$$
$$\text{and} \quad \sigma_f(Pu^{239})/\sigma_f(U^{235}).$$

The computed ratio $\sigma_f(Pu^{240})/\sigma_f(Np^{237})$ varies

TABLE XVII

Values of the Nuclear Parameters Obtained in the Successive Stages of the Reduction of Reactivity Coefficient Data to ν

A. Observed central reactivity coefficient ratios, $\Delta k_o(x)/\Delta k_o(U^{235})$, of isotope x to isotope U^{235} in Topsy, Godiva, and Jezebel.

Isotope x	Topsy	Godiva	Jezebel
Pu^{239}	1.932 ± 0.015	1.910 ± 0.015	1.979 ± 0.015
U^{233}	1.721 ± 0.015	--	1.689 ± 0.020
Pu^{240}	1.37 ± 0.06	1.14 ± 0.11	1.29 ± 0.06
Np^{237}	0.84 ± 0.04	--	0.98 ± 0.02
U^{238}	0.128 ± 0.005	0.163 ± 0.005	0.142 ± 0.005

B. Inferred net production cross-section ratios, $\left[(\nu-1-\alpha)\sigma_f\right]_x/\left[(\nu-1-\alpha)\sigma_f\right]_{U^{235}}$.

Isotope x	Topsy	Godiva	Jezebel
Pu^{239}	1.923 ± 0.015	1.913 ± 0.015	1.947 ± 0.019
U^{233}	1.726 ± 0.015	--	1.664 ± 0.023
Pu^{240}	1.33 ± 0.06	1.11 ± 0.11	1.284 ± 0.06
Np^{237}	0.81 ± 0.04	--	0.98 ± 0.02
U^{238}	0.106 ± 0.008	0.124 ± 0.012	0.175 ± 0.012

C. Inferred ratio, $\left[\nu-1-\alpha\right]_x/\left[\nu-1-\alpha\right]_{U^{235}}$, of excess neutrons produced per fission.

Isotope x	Topsy	Godiva	Jezebel
Pu^{239}	$1.390 \pm 0.03_0$	$1.358 \pm 0.03_0$	$1.330 \pm 0.03_0$
U^{233}	$1.121 \pm 0.03_5$	--	$1.094 \pm 0.03_6$
Pu^{240}	1.89 ± 0.11	1.46 ± 0.16	1.45 ± 0.09
Np^{237}	1.04 ± 0.07	--	0.98 ± 0.05
U^{238}	0.76 ± 0.06	0.80 ± 0.08	0.87 ± 0.06

D. Inferred values of $\left[\nu-\alpha\right]_x$.

Isotope x	Topsy	Godiva	Jezebel
U^{235}	2.47 ± 0.06	2.48 ± 0.06	2.53 ± 0.06
Pu^{239}	3.04 ± 0.09	3.01 ± 0.09	3.03 ± 0.09
U^{233}	2.65 ± 0.08	--	2.67 ± 0.08
Pu^{240}	3.77 ± 0.19	3.16 ± 0.24	3.21 ± 0.16
Np^{237}	2.53 ± 0.12	--	2.50 ± 0.10
U^{238}	2.12 ± 0.10	2.18 ± 0.13	2.33 ± 0.11

E. Inferred values of $\nu(x)$.

Isotope x	Topsy	Godiva	Jezebel	Ave.	$\bar{E}$(Mev)
U^{235}	2.59 ± 0.06	2.59 ± 0.06	2.63 ± 0.06	2.60 ± 0.06	1.45
Pu^{239}	3.10 ± 0.09	3.07 ± 0.10	3.08 ± 0.09	3.08 ± 0.09	1.58
U^{233}	2.70 ± 0.08	--	2.72 ± 0.08	2.71 ± 0.08	1.45
Pu^{240}	3.88 ± 0.20	3.26 ± 0.24	3.27 ± 0.17	3.6 ± 0.5	2.13
Np^{237}	2.62 ± 0.13	--	2.57 ± 0.11	2.60 ± 0.11	2.08
U^{238}	2.61 ± 0.10	2.61 ± 0.13	2.61 ± 0.11	2.61 ± 0.10	3.01

less than one per cent over the grossly different spectra of Topsy, Godiva, and Jezebel. Its uncertainty is thus governed almost exclusively by the uncertainties in the basic cross-section measurements of $\sigma_f(E, Np^{237})$ (*17*) and $\sigma_f(E, Pu^{240})$ (*18*) which should amount to ~4%. We have used

$$\sigma_f(Pu^{240})/\sigma_f(U^{235}) = [\sigma_f(Pu^{240})/\sigma_f(Np^{237})]_{\text{computed}} \times [\sigma_f(Np^{237})/\sigma_f(U^{235})]_{\text{observed}}$$

The computed ratio $\sigma_f(U^{233})/\sigma_f(U^{235})$ again varies less than one per cent over the Topsy, Godiva, and Jezebel spectra, and its estimated 3% uncertainty arises in the measurements of $\sigma_f(E, U^{233})$ and $\sigma_f(E, U^{235})$ (*18*). This computed ratio, however, is ~6% less than the observed ratio (*19*) which, in turn, has an estimated uncertainty of $3\frac{1}{2}$%. The computed value $\sigma_f(U^{233})/\sigma_f(U^{235}) =$

TABLE XVIII

Partial Listing of the Computational Basis for the Estimation of $\bar{\nu}$ Values

	Multigroup representations					
Energy grouping (Mev)	0 - 0.1	0.1 - 0.4	0.4 - 0.9	0.9 - 1.6	1.6 - 3.0	3.0 - ∞
ϕ (Topsy)	0.038	0.233	0.251	0.140	0.221	0.119
ϕ (Godiva)	0.030	0.198	0.255	0.151	0.239	0.127
ϕ (Jezebel)	0.023	0.137	0.214	0.164	0.284	0.178
ϕ^+(Topsy)	1.388	1.109	0.928	0.932	0.989	1.063
ϕ^+(Godiva)	1.431	1.131	0.949	0.951	0.975	1.039
ϕ^+(Jezebel)	1.159	0.976	0.920	0.958	1.013	1.082
$\sigma_f(U^{235})$	2.34	1.43	1.20	1.22	1.22	1.21
$\sigma_f(U^{233})$	3.23	2.24	1.94	1.89	1.83	1.75
$\sigma_f(Pu^{239})$	2.05	1.67	1.70	1.83	1.95	1.90
$\sigma_f(Pu^{240})$	0	0.05	0.77	1.39	1.54	1.60
$\sigma_f(Np^{237})$	0	0.07	0.95	1.63	1.72	1.63
$\sigma_f(U^{238})$	0	0	0	0.044	0.485	0.616
$\sigma_{n,\gamma}(U^{238})$	0.32	0.13	0.113	0.11	0.05	0.02

	Integral representations			
Critical assembly:	Topsy	Godiva	Jezebel	Reference
$\sigma_f(U^{233})/\sigma_f(U^{235})$ Observed	1.630 ± 3 1/2%	1.627	1.610	(5,19)
(Computed)	1.537	1.536	1.527	
$\sigma_f(Pu^{239})/\sigma_f(U^{235})$ Observed	1.391 ± 2%	1.415	1.481	(5,20)
(Computed)	1.384	1.404	1.444	
$\sigma_f(Np^{237})/\sigma_f(U^{235})$ Observed	0.781 ± 3%	0.864	0.996	(5,19)
(Computed)	0.794	0.869	0.994	
$\sigma_f(U^{238})/\sigma_f(U^{235})$ Observed	0.139 ± 2%	0.155	0.200	(5,20)
(Computed)	0.143	0.156	0.201	
$\sigma_{n,\gamma}(U^{238})/\sigma_f(U^{238})$ Observed	0.530 ± 4%	0.476	--	(20)
(Computed)	0.531	0.475	0.335	

1.521 for the U^{235} thermal fission neutron spectrum, however, is ~5% higher than Richmond's measurement of 1.45 ± 2.2% (as quoted by Allen and Henkel (*18*). We adopt the computed ratio; i.e., the implication of the $\sigma_f(E, U^{233})$ and $\sigma_f(E, U^{235})$ data, and assign to it a 3% probable error.

As may be seen in Table XVIII, the computed ratio $\sigma_f(Pu^{239})/\sigma_f(U^{235})$, with an estimated 3% uncertainty, agrees well with the measured value (*20*) which has an estimated 2% uncertainty. The computed ratio for the U^{235} thermal fission neutron spectrum agrees well with Richmond's (*18*) value of 1.423 ± 2.1%. We adopt the mean of the observed and computed ratios listed in Table XVIII, and assign a 2% probable error.

The quantities $[\nu - 1 - \alpha]_x/[\nu - 1 - \alpha]_{U^{235}}$ obtained by division of $\sigma_p(x)/\sigma_p(U^{235})$ by $\sigma_f(x)/\sigma_f(U^{235})$ are listed in Table XVII with their associated probable errors.

C. Absolute Values of $[\nu - \alpha]_x$

According to one-group neutron transport theory, the critical radius of Godiva establishes a relation between the net neutron production cross-section $\sigma_p(U^{235})$ and the transport cross section, $\sigma_{tr}(U^{235})$. $\sigma_{tr}(E, U^{235})$ has been measured throughout the relevant energy range (*18*) with a precision of 5% or better. As may be found, for example, from the extrapolated end point method applied to Godiva, a ~5% uncertainty in the scale of $\sigma_{tr}(U^{235})$ reflects a ~2.3% uncertainty in $\sigma_p(U^{235})$ while the 0.2% uncertainty in the specification of the Godiva critical radius yields a 0.3% uncertainty in $\sigma_p(U^{235})$. It thus appears that the Godiva critical radius and available $\sigma_{tr}(E, U^{235})$ data permit the determination of $\sigma_p(U^{235})$ with a precision of ~2.3%. Present computational techniques, however, cannot fully exploit this possible precision, primarily because of the weak sensitivity of critical radius to weightings of the differential scattering cross sections, $\sigma_s(E, \theta, U^{235})$ other than the transport weighting (it should be mentioned that uncertainties in spectrum-determining parameters such as $\sigma^{in}(E, E', U^{235})$ are of little significance in this connection). We have used the S_n method (*21*) in the S_4 and transport approximations with six-group nuclear parameter descriptions of U^{235} and U^{238} (*22*) for computation of the Godiva critical radius (and for the central values of ϕ and ϕ^+ listed in Table XVIII): this computed radius is

0.3% less than the observed Godiva radius. Here the S_4 approximation yields critical radii 0.8% less than S_∞ (see, for example, Table 2a of reference *17*), while the transport approximation is estimated to produce an additional negative bias of ~0.4%. The nuclear parameter descriptions of U^{235} and U^{238} of reference *18* thus imply a Godiva critical radius 0.9% larger than that observed. To secure agreement we must raise the correspondingly implied value $\sigma_p(U^{235}) = 1.879$ barns by 1.3%. We conclude that the observed critical radius of Godiva implies $\sigma_p(U^{235}, \text{Godiva}) = 1.90 \pm 0.05$ barns, or combined with $\sigma_f(U^{235}, \text{Godiva}) = 1.289 \pm 3\%$ barns, implies $(\nu-\alpha)_{U^{235},\text{Godiva}} = 2.48 \pm 0.06$.[4] If we normalize to this value, $(\nu-\alpha)_{U^{235},\text{Topsy}} = 2.468 \pm 0.06$ and $(\nu-\alpha)_{U^{235},\text{Jezebel}} = 2.526 \pm 0.06$, and thence from our $(\nu-1-\alpha)_x/(\nu-1-\alpha)_{U^{235}}$ ratios the values of $(\nu-\alpha)_x$ listed in Table XVII.

D. Absolute Values of $\nu(x)$

Capture to fission ratio data for the critical assemblies exist only for U^{238}. Here, the observed $\sigma_{n,\gamma}/\sigma_f$ values listed in Table XVIII together with the observed Godiva value $\sigma_{n,2n}(U^{238})/\sigma_f(U^{238}) = 0.05$ (*20*) give the $\nu(U^{238})$ values listed in Table XVII. The available differential (*23*) and/or integral (*24*) $\sigma_{n,\gamma}$ data for U^{235} and Pu^{239} permit estimation of $\alpha(U^{235})$ and $\alpha(Pu^{239})$ in each critical assembly with a ~25% precision. No fast radiative capture data are available for U^{233}, Pu^{240}, and Np^{237}. Nevertheless, the data for other elements suggest that the fast radiative capture cross sections of the heavy elements are similar and it is felt that the error incurred by our assigning to U^{233}, Pu^{240}, and Np^{237} the capture cross sections of U^{238} is only ~50%. Comparison of the $\nu(x)$ and $(\nu-\alpha)_x$ listings of Table XVII indicates the relative unimportance of refining α estimates. Generally, the spread in ν values obtained from reactivity measurements in the different fast critical assemblies is small compared to the stated uncertainties indicating that these uncertainties originate mainly in the estimation procedure. The one exception is for $\nu(Pu^{240})$: here the basic reactivity coefficient measurements were made in Godiva and Jezebel with the same Pu^{240}-enriched plutonium sample whereas the measurements in Topsy involved a separate set of Pu^{240}-enriched samples. We have been unable to determine which was incorrectly specified, and have, therefore, increased the estimated uncertainty in the value of the average $\nu(Pu^{240})$ also listed in Table XVII. In this table, the energy $\bar{E}(x)$ corresponds to the average energy of the critical assembly neutrons producing fissions in sample x and is computed as

$$\bar{E}(x) = \frac{\int E\,\sigma_f(x,E)\sum_i \phi_i(E)\,dE}{\int \sigma_f(x,E)\sum_i \phi_i(E)\,dE}$$

where the summation extends over the assemblies in which reactivity coefficients of x were measured.

[4] Similar procedure utilizing the Jezebel critical size gives $\sigma_p(Pu^{239}, \text{Jezebel}) = 3.72 \pm 0.06$ barns, or with $\sigma_f(Pu^{239}, \text{Jezebel}) = 1.83 \pm 3\%$ barns, gives

$$(\nu-\alpha)_{Pu^{239},\text{Jezebel}} = 3.03 \pm 0.07.$$

REFERENCES

1. G. A. Linenberger, J. D. Orndoff, and H. C. Paxton, *Nuclear Sci. and Eng.* **7**, 44–57 (1960).
2. J. D. Orndoff, *Nuclear Sci. and Eng.* **2**, 450–460 (1957).
3. R. H. White, *Nuclear Sci. and Eng.* **1**, 53–61 (1956).
4. R. E. Peterson and G. A. Newby, *Nuclear Sci. and Eng.* **1**, 112–125 (1956).
5. G. A. Jarvis, G. A. Linenberger, J. D. Orndoff, and H. C. Paxton, Two plutonium-metal critical assemblies. *Nuclear Sci. and Eng.* **8**, 525 (1960). This issue.
6. G. E. Hansen and C. Maier, Perturbation theory for fast-neutron systems. *Nuclear Sci. and Eng.* **8**, 515 (1960). This issue.
7. C. C. Byers, Cross sections of various materials in the Godiva and Jezebel critical assemblies. *Nuclear Sci. and Eng.* **8**, 608 (1960). This issue.
8. R. D. Smith and J. E. Sanders, *Proc. 2nd Intern. Conf. Peaceful Uses Atomic Energy, Geneva* **12**, 89–118 (1958).
9. D. B. Hall and J. H. Hall, Average effective cross sections for the fast plutonium reactor spectrum. Los Alamos Scientific Laboratory Report LAMS-734 (1948).
10. D. J. Hughes, W. D. B. Spatz and N. Goldstein, *Phys. Rev.* **75**, 1781–1787 (1949).
11. D. J. Hughes and J. A. Harvey, Neutron cross sections. Brookhaven National Laboratory Report BNL 325, 2nd ed., U. S. Government Printing Office (1958).
12. G. E. Hansen, H. C. Paxton and D. P. Wood, Critical masses of oralloy in thin reflectors. Los Alamos Scientific Laboratory Report LA-2203 (1958).
13. R. B. Leachman, *Proc. 2nd Intern. Conf. Peaceful Uses Atomic Energy, Geneva* **15**, 331–343 (1958).
14. G. E. Hansen, Thorium-U^{233} Symposium, Brookhaven National Laboratory Report BNL 483, pp. 75–76 (1958).
15. J. Terrell, Conference on the Physics of Breeding, Argonne National Laboratory ANL-6122 (1959).
16. L. Cranberg and J. Levin, *Phys. Rev.* **109**, 2063–2070 (1958).

17. R. B. MURRAY AND H. W. SCHMITT, *Phys. Rev.* **115,** 1707–1712 (1959).

18. W. D. ALLEN AND R. L. HENKEL, "Progress in Nuclear Energy," Ser. 1, Vol. 2, pp. 1–50. Pergamon, New York, 1958.

19. G. A. LINENBERGER AND L. L. LOWRY, Neutron detector traverses in the Topsy and Godiva critical assemblies. Los Alamos Scientific Laboratory Report LA-1653 (1953).

20. C. I. BROWNE, private communication.

21. B. G. CARLSON AND G. I. BELL, *Proc. 2nd Intern. Conf. Peaceful Uses Atomic Energy, Geneva* **16,** 535–549 (1958).

22. G. E. HANSEN, *Proc. 2nd Intern. Conf. Peaceful Uses Atomic Energy, Geneva* **12,** 84–88 (1958).

23. B. C. DIVEN, J. TERRELL, AND A. HEMMENDINGER, *Phys. Rev.* **109,** 144–150 (1958).

24. D. OKRENT, R. AVERY AND H. H. HUMMEL, *Proc. 1st Intern. Conf. Peaceful Uses Atomic Energy, Geneva* **5,** 347–363 (1955).